DELINEATING THE MODE OF ACTION USED BY LITHIUM IN MODULATING OXIDATIVE STRESS AND INFLAMMATION IN ACTIVATED MACROPHAGE CELLS

by

Makola Raymond Tshepiso

Research dissertation submitted in partial fulfilment of the requirements for the degree of

Master of Science

in

Biochemistry

in the

FACULTY OF SCIENCE AND AGRICULTURE

(School of Molecular and Life Sciences)

at the

UNIVERSITY OF LIMPOPO

Supervisor: Dr T.M. Matsebatlela

Co- supervisor: Dr V.G Mbazima

DECLARATION

I declare that the dissertation hereby submitted to the University of Limpopo, for the degree of Master of Science in Biochemistry has not previously been submitted by me for a degree at this or any other university; that it is my work in design and in execution, and that all materials contained herein has been duly acknowledged.

Mr RT Makola

Date

DEDICATION

I dedicate this work to my Father, the late Mr Kgalagadishe Solomon Makola, for he has motivated and showed me how imperative education is. He had a dream of a better life and education, for that matter he has dedicated his life time to make sure everybody around him live that dream, which he failed to get due to his family background.

ACKNOWLEDGEMENTS

The list below represents people whom contributed in one way or another towards the success of this work/ project.

1. Dr TM Matsebatlela, Dr VG Mbazima and Prof MP Mokgotho, for dedicating their time and resources to make this project yield remarkable results.
2. My academic sister Miss Matlotsana Carol Pilane for encouraging me in challenges we encounter in research and help in some of the techniques in Biochemistry.
3. The NRF and University of Limpopo for their financial support
4. My parents and siblings for their constant support
5. My Lovely Girlfriend Kholofelo Seloga for her everlasting support, courage and Love.

Above all I thank the All Mighty GOD of mount Zion for everything He has done possible

TABLE OF CONTENT

LIST OF FIGURES

LIST OF TABLES

LIST OF ABBREVIATIONS

LPS, Lipopolysaccharide; H_2DCF-DA, 2',7'-dichlorodihydrofluorescein diacetate; RHD, rel homology domain; FMLP, N-Formyl-Met-Leu-Phe; PMA, phorbol 12-myristate 13-acetate; PSN, penicillin, streptomycin and neomycin; FBS, Fital Bovine Serum; DAF-2DA, 5,6-Diaminofluorescein diacetate; GSK-3 Glycogen Synthase Kinase-3; NF-κB, nuclear factor-kB; MTT, 3-(4,5-dimethylthiazol-2-yl)-2,5 diphenyltetrazolium bromide; IκB-α, Inhibitor of kappaB kinase alpha; TRAF3, Tnf receptor-associated factor 3; Tollip, Toll interacting protein; Tcf-Lef, T-cell factor-lymphoid enhancing factor; ROS, reactive oxygen species; FDA, US Food and Drug Administration; MØ, Macrophages; γ-GCS, γ- glutamylcysteine synthetase;

ABSTRACT

Lithium is an FDA-approved psychiatric drug that has been used for more than half a century as a preferred, gold standard treatment for bipolar disorders (Cade, 1949; Freland and Beaulieu, 2012). Numerous studies reported that lithium can play a key role in regulation of inflammation and oxidative stress beyond bipolar disorders since it's known to target GSK3-β and NF-κB key inflammation molecules (Yestevelasco *et al*., 2008; Zhang *et al.,* 2008). The choice of this drug was derived from its easy accessibility, less cost, minor side effects and efficacy as opposed to other anti-depressant drugs used currently. This study is based on a body of experimental evidence that has outlined the link between uncontrolled inflammation and some chronic ailments. Thus, this study was aimed at investigating the molecular mode of action of lithium chloride on amelioration of oxidative stress and inflammation in activated Raw 264.7 since, preliminary results of this work suggested the anti-inflammatory properties of lithium. Lithium chloride (LiCl) is not cytotoxic to Raw 264.7 and NIH 3T3 cell lines up to 20 mM and no change in cell proliferation, viability, growth, and cell adhesion were observed as demonstrated using xCELLigence Real Time Cell Analyser (RTCA) and MTT assays. In addition, this drug was shown to be unable to induce programmed cell death in Raw 264.7 and NIH 3T3 cell after 10 mM LiCl treatment as demonstrated using Annexin-V/ PI apoptosis detection assay. Using the Griess and DAF2-DA assays pre-treatment with low doses of lithium (LiCl) was shown to reduce Nitric Oxide production in LPS-induced macrophages. A reduced internal H_2DCF-DA fluorescence intensity is indicative of reduced ROS production, observed in lithium-treated Raw 264.7 macrophages stimulated with LPS, FMLP and PMA. Real Time PCR analysis revealed that lithium modulates expression of inflammation inhibitory genes such as IκB-α, TRAF3, Tollip and NF-κB1/p50. This inhibitors are known to play a vital role up stream (Tollip and TRAF3) and downstream (IκB-α and NF-κB1/p50) of NF-κB inflammation signalling pathway. Thus, these molecules are thought to be anti-inflammatory molecular targets of lithium. Moreover, immunocytochemistry suggest that lithium blocks nuclear translocation of NF-κB. This study associates lithium to reduced oxidative stress in LPS, FMLP and PMA-activated Raw 264.7 macrophages in a non-neuronal setting and further suggests lithium as a potential candidate for regulation of oxidative stress conditions beyond bipolar disorders.

CHAPTER ONE

INTRODUCTION

1.1 Background

Lithium is an FDA approved drug that has been medically used since 1949, as a gold standard psychiatric drug. This alkali metal's reactivity is contributed by its valence electron (Strunecka *et al*., 2005). Over the past five decades lithium has been used as one of the effective mood stabilizers in patients with manic and bipolar disorders (Cade, 1949). Lithium has reduced need for hospitalization through prevention of manic episodes in individuals with bipolar disorder, depression, schizophrenia, and cyclothymia (Birch *et al*., 1993). Despite lithium's preference and significance as a psychiatric drug, its exact mechanism of action is poorly understood (Freland and Beaulieu, 2012).

Nonetheless, both *in vitro* and *in vivo* studies demonstrate that lithium interferes with several significant bio-processes which include receptor mediated signalling, ion transport, hormone and circadian regulation, inflammatory signalling pathways and gene expression patterns (Strunecka *et al*., 2005; Lenox and Wang, 2003). Lithium is thought to exert most of its effects on several bio-processes through inhibition or activation of vital enzymes such as inhibition of inositol monophosphatase (IMPase), inositol polyphosphate 1-phosphatase (IPPase), bisphosphate3-nucleotidase (BPNT1), Fructose 1, 6 bisphosphate (FBPase), Nuclear factor –E2 factor 2(Nrf 2), cyclooxygenase (COX) and GSK-3β (Freland and Beaulieu, 2012).

It is thus inferred that lithium inhibits or activates these enzymatic activities partly because it has a similar radius with enzyme co-factors such as magnesium (Quiroz *et al*., 2004). Moreover, lithium is suggested to possess neuroprotective properties through GSK-3β and NF-κB inhibition, up-regulation of Bcl-2, down regulation of p53, inhibition of c-Jun N-terminal kinase (JNK), stabilisation of apoptosis inducing factor (AIF) and modulation of PI3K/Akt and Wnt anti-apoptotic signalling pathways (Candé *et al*., 2002; Sinha *et al*., 2004; Yeste-velasco *et al*., 2008). Thus, the inhibition/activation phenomenon shown by lithium is thought to be the mechanism in which lithium alters cell signalling pathways and gene expression pattern (Williams and Harwood, 2000). Despite lithium's anti-manic properties, its involvement in

several bio-processes has generated interest in investigating its potential as chemotherapeutic agent.

Neurocognitive impairment is the major problem in that it reduces the quality of life after chemotherapy and radiotherapy. The mechanism used in chemotherapy for inhibition of cancer growth is through suppression of cell proliferation, which as well lowers neurogenesis, eliciting mood and cognitive disorders. In addition to chemotherapy, cranial irradiation has been shown to reduce neural proliferation. Radiation has been observed to mediate neurocognitive impairment by affecting glial cells, neural stem, progenitor cells and the vascular structure. On the other hand lithium has been shown to ameliorate the sequelae emanating from cancer therapy. Neuro-imaging research that includes 3-D magnetic resonance imaging and brain segmentation has shown that lithium repairs damaged brain cells (Khasraw *et al.,* 2012).

Lithium modulates the increment of grey matter and hippocampal volume in patients with bipolar disorders. Furthermore, it protects irradiated neurons from apoptosis in mice thereby improving learning and memory function (Khasraw *et al.,* 2012). Glycogen synthase kinase-3 has been shown to play an essential role during brain development and it's thought to be the molecule which lithium targets to protect neuronal cells from apoptosis (Khasraw *et al.,* 2012). Lithium inhibits GSK-3β leading to the activation of β-catenin which translocates to the nucleus and binds to Tcf-Lef family of transcriptions factors. This family of transcription factors induces expression of Tcf-Lef target genes such as cyclin-D1 and insulin-like growth factor-II (IGF-II). Tcf-Lef genes, specifically IGF-II, induce activation PI3K/Akt survival pathway that gives lithium its neurotoprotective and proliferative characters (Freland and Beaulieu, 2012).

In addition to neuroprotective abilities of lithium, recent findings have suggested that lithium is selectively cytotoxic in that it only induces apoptosis in cancerous cells (HL-60) while sparing noncancerous cells (Matsebatlela *et al.,* 2000). Moreover, lithium is suggested to increase the expression level of heat shock protein (GRp78), thereby lowering mis-folding of proteins, and cytotoxic protein aggregation associated with Alzheimer's disease (Allagui *et al*., 2008; Yeste-velasco *et al*., 2008).

Lithium is known to play a central role in cell metabolism, proliferation and differentiation in various cell types, moreover it stimulates hematopoiesis (Barr and Galbraith, 1983; Allagui *et al*., 2008). Thus, this study focuses on the use of lithium as an anti-inflammatory drug with minor side effects as opposed to other drugs in clinical use. This study emanated from a solid body of evidence that show a link between cancer and other chronic diseases like diabetes, atherosclerosis, bipolar and neurodegenerative disorders and oxidative stress or uncontrolled production of reactive oxygen species (ROS) and reactive nitrogen species (RNS) (Reuter *et al*., 2010). The other underpinned reason is that anti-inflammatory drugs have shown beneficial outcomes in cancer treatment (Reuter *et al*., 2010).

1.2 Cancer and reactive oxygen species

Neoplastic disorders are the most prevalent and severe diseases that afflict a huge number of the population worldwide. These diseases arise from uncontrolled cell proliferation which leads to malignant tumours. Cancer is said to be elicited by several internal and external mutagens such as free radicals (reactive oxygen and nitrogen species), excessive alcohol uptake, tobacco smoking, obesity, ionizing and non-ionizing radiation. These agents alter the cell cycle control points leading to uncontrolled cell cycle and tumorigenesis. The international agency of research on cancer (IARC) reported 12.7 million new cancer cases in 2008 and 4.8 million estimated mortality rate in developing countries (Ferlay *et al*., 2008). Poor quality of life, lack of proper cancer prevention and treatments are suggested to contribute extensively to upraised new cancer cases and mortality in developing countries (Ferlay *et al*., 2008).

Recent line of evidence is pointing towards the involvement of ROS and RNS in a wide variety of disorders including cancer initiation and progression (Reuter *et al*., 2010). Reactive oxygen species are generated in trace amounts as metabolic by-products during mitochondrial respiratory chain (Reuter *et al*., 2010). Excess production of ROS occurs mainly during an immune response to an external or internal injurious agent during a process known as inflammation. Inflammation is phylogenetically and ontogenetically (Ross *et al.,* 2002) the oldest defence mechanism that is controlled by cytokines, products of the plasma enzyme systems,

lipid mediators released from different cells, and vasoactive mediators released from mast cells, basophils, platelets and macrophages (Ross *et al.,* 2002).

Phagocytic cells (e.g. macrophages) were thought to be the only cells that produce ROS during inflammation for the host defence, but other studies (Hancock *et al*., 2001) reported that ROS are also produced by mesangial cells, endothelial cells, osteoclasts and chondrocytes in low amounts (Hancock *et al*., 2001). Macrophage cells produce pro-inflammatory cytokines (interleukin-1β, TNF-*α,* IFN-*γ* and interleukin 6), chemokine and adhesion molecule (E-selectin) at the onset of inflammation to recruit other cells to the site of inflammation, and anti-inflammatory cytokine such as interleukin-10 (IL-10) and interleukin-4 (IL-4) to drive back the inflamed condition in order to regulate inflammation (Peakman and Vergani, 1997; Valko *et al*., 2007). Thus, a larger group of diseases or disorders are related to or caused by dysregulation of the innate immune response and uncontrolled production of reactive oxygen species (Jope *et al*., 2006).

Albeit inflammatory mediators are important during acute inflammation, aberrant production of ROS leads to oxidative stress characterised by an imbalance between oxidants and anti-oxidants. During this condition deformation of cellular components occurs leading to cell demise and development of diseases (Jope *et al*., 2006). Reactive oxygen species consist of a single reactive unpaired electron that denatures proteins, lipids and nucleic acids. Other studies reported that superfluous ROS and RNS influence angiogenesis, proliferation and tumorigenesis by degrading IκB-α (NF-κB inhibitor) (Barnes and Karin, 1997; Reuter *et al*., 2010). Removal of NF-κB inhibitor sequesters NF-κB in the nucleus which promotes expression of angiogenic and survival genes that are thought to promote cancer cell proliferation. This evidence is in line with reports that persistent expression of NF-κB is associated with chronic inflammation, colon, breast and pancreatic cells malignancy (Barnes and Karin, 1997; Reuter *et al*., 2010).

1.3 Oxidative stress

Oxidative stress is a condition where the oxidants overwhelm the antioxidant protective system. This condition occurs when production of oxidants outweighs the production of antioxidants such as superoxide dismutase, glutathione peroxidase and catalase as well as the non-enzymatic antioxidants such as glutathione, vitamin

C, E and D (Reuter *et al*., 2010). Superoxide (O_2^-) is the primary ROS generated through reduction of oxygen (O_2) by NADPH oxidase during mitochondrial respiratory chain. Thereafter, other ROS like hydrogen peroxide (H_2O_2) are generated by an enzyme superoxide dismutase (Reuter *et al*., 2010). Studies (Barnes and Karin, 1997; Jope *et al.,* 2006) have outlined the link between oxidative stress and chronic ailments with prolonged activation of AP-1, NF-κB and GSK-3β, the vital inflammatory mediators.

These molecules are known to be harmless in trace amounts with beneficial properties such as their role in wound healing and cellular signalling pathways as second messengers (Reuter *et al*., 2010). During oxidative stress, excess H_2O_2 generate vast other toxic ROS like hydroxyl ions (HO^-), which are generated from H_2O_2 through fenton reaction in the presence of reduced metal (Cu, Fe and Ni) (Figure 1a). Hydroxyl ions are the most reactive species that damages DNA through generation of 8-hydroxydeoxyguanosine which is known to be a radical attack biomarker (Figure 1b) (Reuter *et al*., 2010). DNA base oxidation can be repaired by several cellular DNA repair systems, but if it occurs at a critical point or its not removed immediately, ROS can cause point mutation, mutation of tumor suppressor genes and DNA strand break. Radical attack leads to genomic instability and transformation of normal cells to tumor cells (Reuter *et al*., 2010).

A. $Fe^{2+} + H_2O_2 \text{ ----> } Fe^{3+} + .OH + OH^-$

$Fe^{3+} + H_2O_2 \text{ ----> } Fe^{2+} + .OOH + H^+$

B.

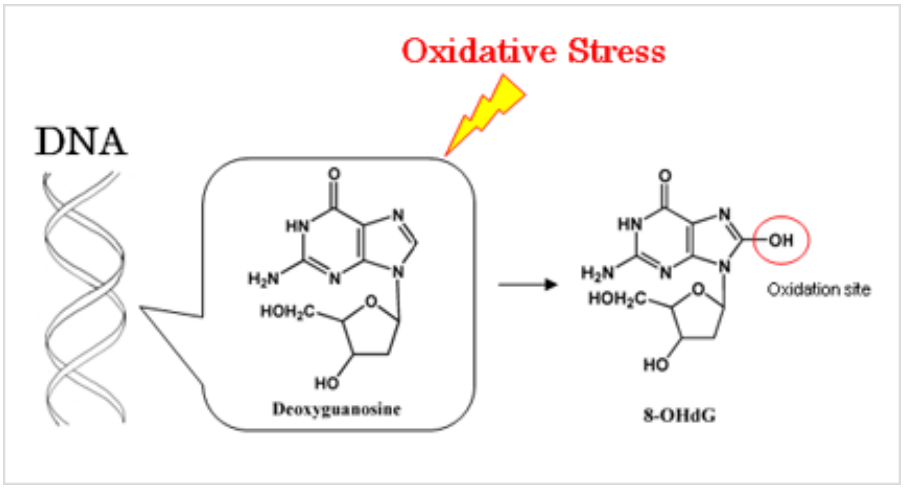

Figure1.1: Schematic representation of a fenton reaction in the presence of a metal ion and DNA radical attack: [A] depicts the generation of vast other free radicals such as hydroxyl ions from hydrogen peroxide during a fenton reaction. [B] shows generation of 8-hydroxydeoxyguanosine as a result of free radicals oxidation that leads to genomic instability (Reuter *et al*., 2010).

Oxidative injury is linked to several diseases such as cancer, atherosclerosis and neurodegenerative diseases such as Alzheimer's disorders (AD) and Parkinson's disease (PD). The oxidative damage is known to target proteins, lipids and nucleic acids resulting in alteration of cell structure and function (Pizarro *et al.,* 2008). Oxidative damage has been recognised in patients suffering from AD, PD and stroke since, neuronal cells consists of low glutathione content and their membranes contain high proportions of polyunsaturated fatty acids. Furthermore, brain metabolism requires high amounts of O_2 thus, maximising exposure of brain cells to oxygen molecules. Lipid peroxidation in the brains of AD patients was reported, especially in the temporal lobe (Christen, 2000). In the arteries, excessive production of ROS leads to oxidative modification of low density lipoprotein (LDL) in the arterial walls.

Oxidation of LDL (ox-LDL) by ROS is thought to cause endothelial dysfunction which is the onset of atherosclerosis. These ROS mainly come from macrophages and smooth muscles in the blood vessels (Vogiatzi *et al*., 2009). Similarly, excessive production of ROS is stimulated in many related disease conditions such as diabetes mellitus, hypercholesterolemia, arterial hypertension, smoking, aging, and nitrate intolerance. Excessive superoxide anion (O_2^-) reduces endothelial derived nitric oxide (NO), the most important endogenous vasodilator, and these results in vasoconstriction, platelets aggregation and adhesion of neutrophils to the endothelium. This condition then causes blood pressure and hypertension. Excessive hydrogen peroxide leads to increased phosphorylation of tyrosine kinases which lead to binding of neutrophil cells and alteration of vessel permeability (Vogiatzi *et al*., 2009).

1.4 NF-κB transcription factor

Rel/NF-κB is a transcription factor that possess a broad spectrum of activity, since it's known to be involved in several signalling pathways namely; inflammation, proliferation, growth, differentiation, apoptosis and angiogenesis (Barnes and Karin, 1997; Moynagh, 2005). The NF-κB transcription factor is predominant within the cytosol in resting cells and complexes with inhibitor of kappa B (IκB) proteins. Initially this transcription factor was known to regulate the expression of kappa light chain genes in murine B lymphocytes recognising 5`-GGGRNNYYCC-3` as a consensus sequence (where R- purine and Y-pyrimidine), hence the name nuclear factor kappa-light-chain-enhancer of activated B cells. However, to date studies (Barnes and Karin, 1997) have recognised Rel/NF-κB family of proteins in almost all animal cells.

Rel/NF-κB is a pleiotropic protein that describes a family of proteins that form dimers, which have a conserved N-terminal, the rel homology domain (RHD) (Figure 2). RHD consist of 300 amino acids (aa) within which lies DNA binding domain, nuclear localisation signal and Dimerisation domain. This domain enables dimerisation of NF-κB subunits, nuclear translocation and binding to kappa responsive site (May and Ghosh, 1997). This family consists of five proteins subunits namely: NF-κb1/p50, NF-κB2/p52, c-Rel, RelA/p65 and RelB that form hetero and/or homo-dimers, which results in an active transcription factor. The IκB are functionally and structurally related family of proteins with centrally located 30-33 aa sequence repeat known as SW16/ ankyrin (Moynagh, 2005).

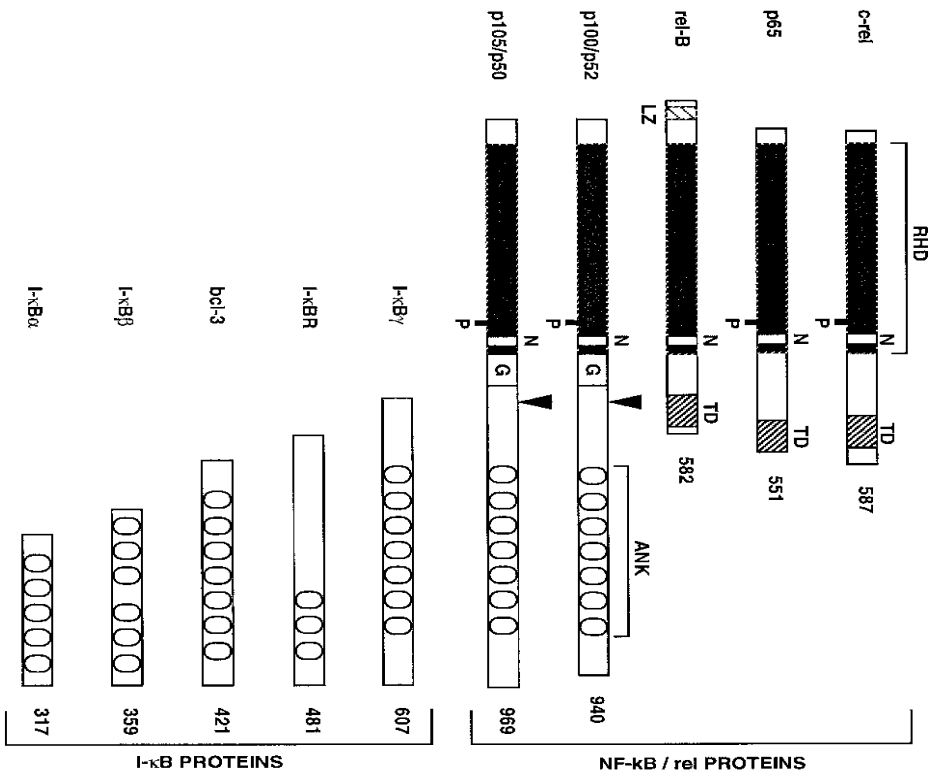

Figure 1.2: Demonstration of the domains and conserved sequences of NF-kB family of proteins. NF-kB family of proteins consist of a number of subunits that dimarise to from a complete transcription factor, these subunits have a conserved N–terminal. Moreover, they are inhibited by a related family of inhibitors that have a conserved 30-33 aa sequence repeat known as SW16/ ankyrin (Moynagh, 2005; May and Ghosh, 1997).

The NF-κB-p50 and p52 precursor proteins, p105 and p100, exhibit the ankyrin repeats at their C-terminal prior processing and they were shown to be capable of inhibiting NF-κB dimers. The IκB family of proteins include IκB-α, IκB-β, IκB-γ, IκB-ε, Bcl-3, IκB-R, p100 and p105 which consist of between three to seven ankyrin repeats that mask the nuclear localisation signal of NF-κB on RHD at the C-terminal (Moynagh, 2005). Inhibition of Rel proteins is accomplished through protein-protein interaction of centrally located ankyrin repeat of IκB and RHD in the Rel dimers. These IκB proteins are known to inhibit specific dimers of the NF-κB, such as p50, p52, c-Rel, Rel-B and Rel-A. IκB-α and β inhibit complexes composed of C-Rel and RelA/p65, Bcl-3 inhibit homodimers of p50 or p52, IκB-γ inhibit C-Rel, p50/p65 and p50 homodimers, and IκB-ε only binds to C-Rel, RelA or their dimers (May and Ghosh, 1997).

Despite the specificity of IκB proteins, the NF-κBp50/p52 precursor proteins show little specificity. The precursors p105 and p100 have been reported to inhibit dimers composed of these subunits; p50, p52, RelA and C-Rel. These precursor proteins are the only molecules that can inhibit RelB. Furthermore, the 46 kDa C-terminal of p100 (named IκB-δ) inhibits p52/RelB heterodimers that induce genes involved in B-cell development (May and Ghosh, 1997). Besides the central located ankyrin the N and C terminal domain of the IκB has been demonstrated to exhibit a significant function. Knocking out of the C-terminal domain does not alter NLS masking abilities of the IκB, rather leads to a loss of its DNA dissociation abilities and the ability to block the DNA-binding of NF-κB (May and Ghosh, 1997).

The C-terminal of IκB consists of an acidic and Thr- rich PEST sequence which is thought to prevent NF-κB DNA-binding activity. The N-terminal contains a site of serine phosphorylation and ubiquitination, which is pivotal for signal induced degradation of IκB (May and Ghosh, 1997). The translocation of NF-κB is achieved by activation of IκB Kinase (IKK) subunits complex composed of (IKK-a, IKK-b) and the regulatory non-enzymetic scaffold proteins IKK-γ/ NEMO (NF-Kappa-B essential modulater). IKK is known to phosphorylate IκB on serine (Ser536 and 529) then followed by the binding of the ubiquitin ligase complex β-TrCP-SCF, which tag IκB for degradation by 26S proteasomes (Moynagh, 2005).

The NF-κB dimer is then sequestered in the nucleus where it binds to its responsive element and enhances transcription (Barnes and Karin, 1997). IκB Kinase is activated by MAPK and TAK-1 after a signal from various stimuli like ligands of Toll-like receptor (TLRs), TNF super family receptors and microbial cytoplasmic receptors, Nod1 and Nod2. Toll-like receptors are messengers of microbial inversion, through recognition of pathogen associated molecular pattern (PAMPs) and then production of pro-inflammatory proteins. The Toll-like receptors share a conserved Toll/IL-1R (TIR) domains and recruit adaptor molecules containing the related domain, adapter proteins such as; Myd88, Mal/TIRAP, TRIF/ TICAM-1 and TRAM/ TACAM-2. These adaptor proteins recruit proteins from IRAK family. IRAK is recruited by Myd88 in association with Toll-interaction proteins (Tollip), therefore this complex lead to hyperphosphorylation of IRAK by IRAK-4. Phosphorylated IRAK dissociate from the Myd88- Tollip- IRAK complex. IRAK interact with TRAF-6 thereby activating downstream TAK1 (Moynagh, 2005).

Furthermore, IRAK promotes the translocation of TAK1-binding protein-2 (TAB2) from the membrane to the cytosol where it interacts with TRAF-6 and bridge the association of TRAF-6 with TAK1, where in which activated TAK1 helped by TAB1 activate IKK complex. The activity of TRAF-6 is dependent on polyubiqutinylation of TRAF-6, which is regulated by tumor suppressor CYDC (a deubiqutinylation enzyme) that inhibits ubiqutinylation of TRAF proteins and activation of NF-κB thereof (Moynagh, 2005).

NF-κB consists of two groups, those that contain C-terminal transactivation domain (TD) such as c-Rel, RelA/p65 and RelB (figure 2). The group of Rel proteins that possesses TD executes transcription as opposed to the Rel proteins that do not possess TD. The TD deficient proteins NF-κb1/p50 and NF-κB2/p52 are produced as precursor proteins p105 and p100 which are degraded to NF-κb1/p50 and NF-κB2/p52. Thus, homo or heterodimers of this group does not induce transcription unless they interact with BCl-3, a proto-oncoprotein that belongs from IκB family. BCl-3 is thought to promote transcription abilities of p50 and/ p52 in two distinct ways; firstly by masking the DNA binding site of this dimers allowing the other transcriptional active dimers to bind and enhance transcription; secondly it's thought to form a DNA binding domain that promotes transcription abilities (May and Ghosh, 1997).

NF-κB has been shown to promote the transcription of inflammatory genes such as: pro-inflammatory cytokines, chemokines, adhesive molecules and inducible enzymes such as nitric oxide synthase and cyclooxygenase-2 (Barnes and Karin, 1997). This suggests that NF-κB plays a central role in inflammation hence the interest of this study in this transcription factor.

1.5 Glycogen Synthase Kinase

Glycogen Synthase Kinase-3 (GSK-3) is a serine/threonine kinase that was first recognised and isolated as an enzyme involved in the regulation of the metabolic enzyme, glycogen synthase (Embi *et al*., 1980). To date, GSK-3 is known to have diverse biological activities such as its involvement in gene expression, inflammation, cellular architecture, apoptosis, cell cycle regulation, growth, differentiation and proliferation (Li *et al.*, 2010). There are two GSK-3 characterised isoform that are encoded by two different genes; GSK-3α and GSK-3β. Glycogen Synthase Kinase-

3α is 51 kDa size, whereas GSK-3β has a mass of 47 kDa. Glycogen Synthase Kinase-3α has glycine-rich extension at the N-terminal that makes it different from GSK-3β. The most defined mechanism of regulating GSK-3 is through direct phosphorylation of a serine residue on either of the two isoforms of GSK-3, serine-9 in GSK-3β and serine-21 in GSK-3α (Jope *et al*., 2007).

The major regulator of GSK-3 is phosphatidylinositol 3-kinase (PI3K)/ Akt signalling pathways as stimulated by various stimuli like insulin. Other known regulators include kinases such as protein kinase C and A which phosphorylate serine residues (Jope *et al*., 2007). Glycogen Synthase Kinase-3 has an unusual preference for target protein that are pre-phosphorylated at a priming residue located at the C-terminal to the site of GSK-3 phosphorylation (Doble and Woodgett, 2003). The consensus sequence that GSK-3 recognise is Ser/Thr- X-X-X-Ser/ Thr-p, where the first serine or threonine is the target residue, X is any amino acid but often proline and the last ser-p/ Thr-p is the site of priming phosphorylation (Doble and Woodgett, 2003).

Lithium has been reported to inhibit GSK-3 directly or indirectly. Direct inhibition involve competitive inhibition since, lithium has the same radius as magnesium (Mg^{2+}) (Quiroz *et al*., 2004). However, indirect inhibition involves induced phosphorylation of GSK at serine-9/ 21 residues by other upstream kinases (Tim *et al*., 2011; Jope *et al*., 2007). Glycogen Synthase Kinase-3 is known to regulate cell signalling pathways such as cell survival, Wnt, receptor tyrosine kinase and G-protein coupled receptor (Doble and Woodgett, 2003). This kinase promotes stimuli-induced production of several cytokines such as IL-6, IL-1β and tumor necrosis factor (TNF), followed stimulation of Toll-like receptor in monocytes macrophages (Jope *et al*., 2007).

Glycogen Synthase Kinase-3β is known to activate NF-κB in a promoter specific manner showing that GSK-3 selectively supports gene expression promoted by NF-κB (Jope *et al*., 2007). This kinase is suggested to be part of tumor suppressor complex due to its direct phosphorylation leading to the degradation of the, oncoprotein, β-catanine. Moreover, GSK-3 is suggested to promote ovarian cancer cells proliferation, where cycline –D is thought to be involved (Cao *et al*., 2006).

1.6 Glutathione

Glutathione (GSH) is a water soluble tripeptide composed of glycine, glutamine and cysteine. This molecule serves as a detoxifying agent, both as a single molecule and as co-factor of enzymes such as GSH S-transferase (GST) and GSH peroxidase (GPx) (Cui *et al*., 2007; Townsend *et al.,* 2003). The GSH cysteine thiol is the nucleophilic reducing agent that reacts with both the exogenous and endogenous electrophilic species (Townsend *et al.,* 2003). The elevated levels of intracellular GSH combat and protect cells from the detrimental ROS, both enzymatically and non-enzymatically. Enzymatically GSH can react with H_2O_2 a reaction catalysed by GPx which results in H_2O and GSH-disulfide (Cui *et al*., 2007).

Glutathione is as well known to conjugate with oxidised products as catalysed by GST to form non-toxic and excretable products (Cui *et al*., 2007). Glutathione is known to exist in vast amounts in living organisms such as animals, plants and some other prokaryotes. Furthermore, it is known for playing a role in the glyoxalase system, reduction of ribonucleotide to deoxyribonucleotide, regulation of proteins and gene expression via thiol; disulphide exchange reaction (Townsend *et al.,* 2003). Glutathione is synthesised *de novo* in a two-step reaction that involve enzymes such as γ- glutamylcysteine synthetase (γ-GCS) and GSH synthetase (Townsend *et al.,* 2003). This involves ligation of glutamate with cysteine as catalysed by γ-GCS resulting in γ-glutamylcyteine. The second reaction step combines this dipeptide with the glycine catalysed by GSH synthase to produce a complete and active GSH (Cui *et al*., 2007; Townsend *et al.,* 2003).

Cysteine was found to be the rate limiting factor which its availability within the cell is conducted by sodium dependent and independent transporters, respectively. Oxidants elevate the cysteine uptake and the γ-GCS expression, where AP-1 was found to be the expression enhancer. This is as a result of the availability of AP-1 binding site on the γ-GCS responsive site (antioxidant responsive element) (Townsend *et al.,* 2003). A line of evidence links neurodegenerative disorders, such as Parkinson's diseases (PD), with oxidative stress that alters cell components and eventually cell dermis (Townsend *et al.,* 2003). The brain is known to be prone to oxidation since, its metabolism requires high amounts of oxygen and it's composed of polyunsaturated fatty acids (Christen, 2010).

This disease condition manifest as a result of destruction of the dopaminergic neurons in the substantia nigra pars compacta (SNpc) midbrain. Parkinson's disease is characterised by deficiency in dopaminergic neuronal cells that are involved in dopamine metabolism. This deficiency is thought to be due to high amounts of H_2O_2, which is generated during dopamine metabolism, which in normal physiology is reversed by GSH. Therefore, the perpetuation of PD is accompanied by depletion of GSH and increment of ROS within the SNpc (Townsend *et al.,* 2003).

1.7 Macrophages

Macrophages (MØ) are phagocytic and antigen presenting cells (APCs) that are known to constitute the first line of defence (innate immune response). Macrophage cells are differentiated from circulating monocytes which are derived from bone the marrow promonocytes. The differentiation of monocytes to a complete differentiated MØ is influenced by growth factors such as Granulocytes macrophage colony-stimulating factor (GM-CSF) and macrophage colony-stimulating factor (M-CSF). These growth factors are known to be lineage growth factors that stimulate differentiation and proliferation of myeloid lineage cells (Peakman and Vergani, 1997; Taylor *et al*., 2005).

Macrophages are known to reside as residential cells in the lymphoid and nonlymphode organs such as liver (kuffer), spleen (white and red pulp MØ), peritoneum (peritoneal MØ), lungs (alveolar macrophages), nervous system (microglia), reproductive organs and serosal cavity (Taylor *et al*., 2005). Macrophages from different microenvironments such as liver and/or lung are phenotypically and functionally different (Xu *et al*., 2006). During inflammatory response other cells from different microenvironments are recruited to the inflamed site by cytokines such as interferon-γ (IFN- γ), interleukin-4 (IL-4) and IL-13 where they display various phenotype and function from their original microenvironment (Taylor *et al*., 2005).

Macrophages express a wide range of plasma receptors that regulate cell differentiation, growth and survival, adhesion, migration, phagocytosis, activation, antigen presentation and cytotoxicity (Taylor *et al*., 2005). These cells are populated at the site of entry from the external environment, such as lungs, where they are exposed to fungi, bacteria and viruses since they are known to constitute the first line

of defence. Thus, alveolar macrophage cells express a variety of plasma membrane receptors such as scavenger receptor (SR), lectin-like receptors, opsonic specific receptors (fc receptors), β-glucan specific receptor and most importantly TLRs (Taylor *et al.,* 2005).

TLRs are known of their divers sensing abilities that include; microbes and other ligands. These receptor molecules are known to mediate signalling via adaptor molecules such as MyD88. Furthermore, antigen recognition specificity and binding affinity is improved by compliment receptors such as CD14 and MD2 (Gordon, 2007; Taylor *et al*., 2005). These compliment receptors are known to be LPS receptor and binding protein in LPS induced response (Gordon, 2007). The expression of each receptor is tightly regulated in monocytes-macrophages, myeloid dendritic cells (DCs) and polymorphonuclear leukocytes (PMN), during their differentiation, migration in to deferent tissue microenvironment and cell activation (Taylor *et al*., 2005).

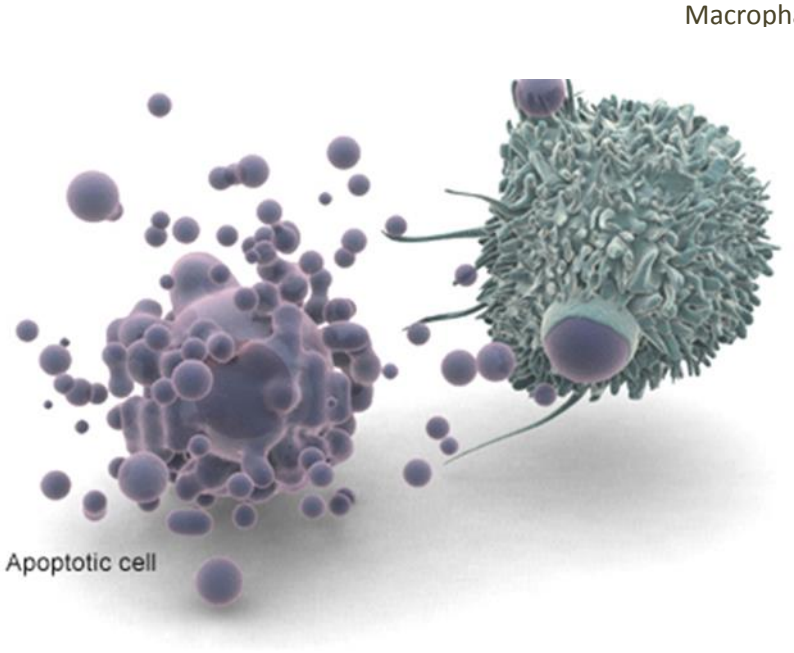

Figure 1.3: The phagocytic macrophage cells mopping off apoptotic bodies from an apoptotic cell. The later phase of apoptosis is determined by apoptotic bodies which are removed by phagocytic cells such as macrophages without eliciting an immune response (Peakman and Vergani, 1997).

Macrophages function as scavenger cells mopping apoptotic cells and old erythrocytes in a silent mode, as opposed to necrotic debris that elicits inflammatory response (figure 3) (Peakman and Vergani, 1997). The phagocytosis of apoptotic cells make use of receptor such as vitronectin receptor (VnR) cooperating with thrombospondin and CD36, LOX-1 that is known to bind aged erythrocytes. Other receptors include the PS binding receptors such as phosphotydil serine receptor (PSR) that recognise phosphotidyl-L-serine and not the D isoform, and sacavenger receptor such as *β*2-GPI Receptor. Furthermore, other molecules reported in apoptotic cell recognition are some complimentary receptors such as complimentary receptor 3 (CR3) and 4 (CR4) and surface proteins A (SP-A) and D (SP-D) (Taylor *et al*., 2005).

During the early phase of apoptosis, the dying cell expose the eat me signal (phosphotidyl serine) that prompt the MØ to engulf and remove them in order to maintain homeostasis and tissue remodelling (Xu *et al*., 2006). The apoptotic eat me signal (PS) is recognised by macrophage cells which are classified in to two subtypes namely MØ1 and MØ2 of which type 1 is known to be pro-inflammatory and type 2 anti-flammatory as influence by GM-CSF and M-CSF, respectively. From these subtypes the MØ2 has been illustrated to have high affinity to clearance of early apoptotic cells as compared to MØ1 (Xu *et al*., 2006). Xu *et al* (2006) suggest that clearance of cells which have undergone apoptosis is more effective with a certain MØ subtype.

The anti-inflammatory MØ-2 subtype is associated with apoptotic cells clearance since it is four times more effective in apoptotic cell clearance than the MØ-1. Macrophage-2 subtype was shown to retain the production of anti-inflammatory cytokine IL-10 and IL-4. In contrast, MØ1 are inhibited from producing the pro-inflammatory cytokines, for which this is believed to be the mechanism in which apoptotic cells are removed in a silent manner (Xu *et al*., 2006). Apart from scavenging abilities shown by MØ, these cells are known to be involved in wound healing. This physiological process is classified into three stages; inflammation, proliferation and regulation. Therefore, macrophages play a major role not only in the initiation phase of inflammatory response, but also in the growth phase via production of angiogenic and fibrogenic growth factors. It is therefore reported that

TLRs 2, 4, 7, 9 and adenosine A (2A) receptor program macrophage to secrete VEGF and other angiogenic factors (Plowden *et al*., 2004).

Macrophages are known to play a vital role in both innate adaptive immune response. The PRM/ PRR found on the surface of phagocytes such as scavenger receptor (SR), lectin-like receptors, opsonic specific receptors (fc receptors), β-glucan specific receptor and TLRs (Taylor *et al.,* 2005) interact with foreign molecules and elicit activation of phagocytosis and enzymes that are involved in the digestion of those molecules (figure 4). Macrophages impart the signal to the adaptive immune response T-lymphocyte, in particular, through their antigen presenting abilities. They present the antigen to T_H Cell in the Lymph node through the protein named class II major histocompatibility complex (MHC II), which embed antigen derived from degraded foreign molecule (Madigan *et al*., 2009).

The T cell interact with MHC II with their T cell receptors, and then differentiate into T cytotoxic cell, T_H cell 1 and T_H cell 2. These T cell initiate immunity, T_H cell 1 activates macrophages to kill engulfed pathogens like *mycobacterium tuberculosis* which can survive in the phagocyte. Moreover, this subset as well activates macrophages and other phagocytic cells to secrete cytokines like: interferon gamma (INF_Y), tumour necrosis factor alpha (TNFα) and GM-CSF that recruit other immune cells. T_H cell 2 activates B cells to secrete antibodies that make it easy for phagocytes to adhere and engulf foreign molecules (Madigan *et al*., 2009).

1.8 Aim

This study aims to investigate the mechanism in which lithium modulates inflammation and oxidative stress in LPS, PMA and FMLP activated macrophages.

1.9 Objectives

The objectives of this study were to determine the:

i) Proliferation and growth profiles of lithium treated RAW 264.7 macrophages by xCELLigence Real Time Cell Analyser**,** MTT viability assay and Cell morphology imaging.

ii) Apoptotic effects of lithium on RAW 264.7 macrophages using Annexin V-FITC/PI apoptosis detection assay and DAPI.

iii) Effects of lithium on reactive nitrogen species production using Griess and Daf2-DA Nitric Oxide measurement assays.

iv) Effect of lithium on expression profiles of several genes that are linked to NF-κB and MAP kinase signalling pathway carried out using Real Time-PCR arrays.

v) Effects of lithium on translocation of NF-κB p65 from cytosol to nucleus using immunohistochemistry.

CHAPTER TWO

MATERIALS AND METHODS

2.1 Cell Culture

Raw 264.7 macrophage cells were obtained from Prof Gordon Brown (institute of infectious diseases and molecular medicines-University of Cape Town) (RSA). The cells were maintained in cell culture flasks at 37^{o}C, in a humidified 95% air and 5% CO_2 atmosphere. Cells were propagated in RPMI-1640 supplemented with 10% FBS, 2 mM L-glutamine and 1x penicillin, streptomycin and neomycin mixture (PSN). The NIH 3T3 fibroblast cells were obtained from ATCC, and were also cultured under the same condition but propagated in DMEM supplemented with 10% FBS, 2 mM L-glutamine and 1x PSN. Determination of cell density was executed using trypan blue exclusion assay. This assay was accomplished by diluting cells with 10x with trypan blue dye, and then cells were counted using hemocytometer under the inverted light microscope.

2.2 Cell Viability and Proliferation

In order to assess effects of lithium chloride (Fluka Chemika, Switzerland) on Raw 264.7 and NIH 3T3 cells proliferation MTT assay was employed. This assay was initiated by seeding cells (Raw 264.7 or NIH 3T3) in a 96 well culture plate at a density of 6 x 10^6 cells/ml, and incubated overnight. Thereafter, Raw 264.7 cells

were treated with various concentrations of LiCl (0.6125, 0.325, 1.25, 2.5, 5, 10, 20, 50 and 100 mM), 10 mM NaCl, and 20 µg/ml actinomycin-D (Sigma Aldrich, USA) for 24 hrs. On the other hand the NIH 3T3 cells were treated with 10 mM LiCl, 10 mM NaCl, and 20 µg/ml actinomycin-D for 24 hrs. Cell imaging was executed with a light microscope prior addition of 5 mg/ml of MTT (Fluka Biochemika, Switzerland) for 4 hrs. After incubation, the cells culture medium was aspirated and 100 µl of solubilising solution DMSO (Saarchem, RSA) was added and incubated for an hour. This was followed by measuring absorbance at 570 nm using GloMax-Multi microplate reader (Promega, USA).

2.3 xCELLigence Real Time Cell Analyser

The real time cell analyser system xCELLigence was utilises in order to monitor the anti-proliferative and cytotoxic effect of LiCl on Raw 264.7 macrophage cells. xCELLigence is a current based cell sensor that relates electrical impedance to cell status/cell index as determined by cell morphology, cell adhesion and cell number. This system was set and initiated according to manufacturer's protocol, thereafter, followed by seeding cells in microelectrical cell sensor arrays at a density of 40 000 cells/well for 24 hrs. The cells were then treated with 20 µg/ml actinomysin-D, 10 mM NaCl and various concentration of LiCl (100, 50, 20, 10, 5, 2.5, 1.25 mM) for 56 hrs. The xCELLigence (RTCA) software was set to takes readings after every 15 minutes interval (Roche, USA).

2.4 Annexin-V FITC, Propidium Iodide (PI) apoptosis detection assay

2.4.1 Qualitative apoptosis detection assay

The apoptotic effects of 10 mM LiCl on Raw 264.7 and NIH 3T3 cells were assessed using Annexin-V FITC/ PI kit (BD-Biosciences, USA) according to manufacturer's protocol. Cells were seeded at a density of 6 x 10^6cells/ml on coverslips in a 6 well plate and incubated overnight. Cells were treated with 10 mM NaCl, 10mM LiCl and 20 µg/ml actinomycin D for 24 hrs. This was followed by removal of medium and washing with 1x PBS. Cells were stained with PI and Annexin-V for 20min in the dark at room temperature (RT). Cells on the coverslips were fixed for 30 min with 3.7% paraformaldehyde. Coverslips where then mounted with mounting medium on

microscope slides and cell imaging was accomplished with Nikon Ti-E inverted fluorescent microscope (Nikon, Japan).

2.4.2 Quantitative apoptosis detection assay

The quantitative analysis of apoptotic effects of 10 mM LiCl was carried with flow cytometer according to manufacturer's protocol (BD Biosciences, USA). This machine distinguishes viable cells from those that are undergoing apoptosis. In order to examine the apoptotic effects of lithium, cells were seeded at a density of 6 x 10^6cells/ml in 60 mm cell culture dishes and incubated overnight. Cells were treated with 10 mM NaCl, 10 and 20 µg/ml actinomycin-D and 5, 10, 20 and 50 mM LiCl and for 24 hrs. This was followed by removal of medium and washing with 1x PBS. Cells were stained with PI and Annexin-V for 20 min in the dark at room temperature (RT), this was then followed by washing and suspending in 1x PBS. Suspended cells were analysed using flow cytometer.

2.5 Griess reagent assay

Griess assay is a calorimetric assay that measures Nitrite (NO_2^-), one of the two primary stable forms of Nitric oxide. This assay relies on reaction described in 1879 by Griess (Griess, 1879). In order to assess the effects of LiCl on nitric oxide (NO) production, cells were seeded in 96-well plates at a density of 6 x10^6 cells/well in a phenol red-free medium overnight. Cells were treated with various concentrations of lithium (1.25, 2.5, 5 and 10 mM LiCl) and 10 mM NaCl as well as the combination of each of these salts with 10 µg/ml LPS (Sigma, USA) for 24 hrs. After 24 hrs of treatment, Nitric oxide was measured by mixing equal amounts of phenol red-free medium and Griess reagent (Sigma-Aldrich, USA). The absorbance was measured using GloMax-Multi microplate reader at 550 nm (Promega, USA).

2.6 Daf2-DA Nitric Oxide measurement assay

Daf2-DA assay is fluorescence based NO detection assay that uses a cell permeable 4, 5-Diaminofluorescein diacetate (DAF2-DA) as NO detector (Sigma-Aldrich, USA). The diacetate (DA) part of DAF2-DA is hydrolysed by cellular esterases to produce DAF2 compound that reacts with NO to produce a fluorescent triazolofluorescein (DAF-2T). Therefore, in this study cells were seeded on coverslips in 6 well plates overnight and then treated with various concentrations

of LiCl (1.25, 2.5, 5 and 10 mM), 10 mM NaCl, 100 ng/ml Ultrapure LPS (Invitrogen, USA) and the combination of each of the chemicals with 100 ng/ml LPS for 24 hrs. Thereafter, cells were stained with 10 µM/ml DAF2-DA for 20 min at RT and washed with 1x PBS. Cells were further stained with 25 µg/ml Hoechst for 20 min at RT, thereafter followed by fixing with 2.7% paraformaldehyde for 30 min. Nitric Oxide quantitation was done with a Nikon Ti-E inverted fluorescent microscope (Nikon, Japan).

2.7 Oxidative burst assay

In an attempt to analyse the effects of lithium on oxidative burst, Phagoburst assay kit (Glycotope, Germany) was utilised according to manufacturer's protocol. This is a fluorescent based assay that uses a fluorigenic cell permeant, H_2DCF-DA that is converted to a highly fluorescent DCF through removal of the acetate groups by intracellular esterases and oxidation. This assay was initiated by transferring cells at a density of 6 x 10^6 cells/ml on cover slips in 6-well plate overnight. Thereafter, cells were treated with 10 mM LiCl and 10 µg/ml LPS for 24 hrs. The other experiment contained cells pre-treated with 10 mM LiCl for 24 hrs and FMLP as well as PMA for 30 min. Thereafter, cells were washed once with wash buffer and then 50 µl of H_2DCF-DA was added in all plates for 30 min in the dark at RT, and then followed washing with wash solution and addition of 50 µl of DNA staining solution for 20 min at RT in the dark. The DNA staining solution was removed and 3.7% paraformaldehyde was added for 30 min to fix the cells. This was followed by mounting coverslips on the microscope slide and examination under Nikon Ti-E inverted fluorescent microscope (Nikon, Japan).

2.8 GSH-Glo Glutathione assay

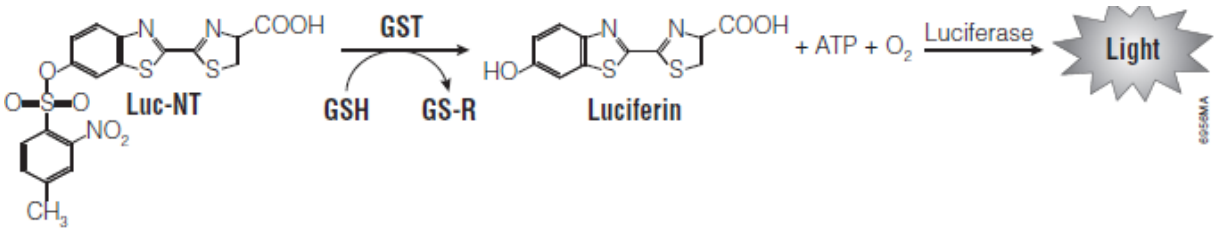

Figure 2.1; Schematic representation of the glutathione detection reaction in the presence GTS and Luciferin-NT. GSH is one of the vital antioxidant that a cell

produce especially the neuronal cells. Thus, this figure depicts the mechanism of measuring GSH using a luminescence base assay.

Glutathione assay is a two-step luminescence based assay that quantifies the level of glutathione. This assay involves the generation of Luciferin from a luminogenic substrate (Luciferin derivative) catalysed by Glutathione S Transferase (GST) in the presence of Glutathione. Step two uses Luciferase to detect the Luciferin produced in the first step, the luminescence generated in the second step is directly proportional to the amount of glutathione produced in each well. In order to measure the level of glutathione, cells were cultured at 1 x 10^4 cells/ml density overnight. Thereafter, cells where treated with 10 mM LiCl and 100 ng/ml ultrapure LPS, 10 µg/ml PMA and 10 µg/ml FMLP. Moreover, other mentioned cells were treated with a combination of LiCl with each of the above mentioned stimulants. The treatment with LiCl and LPS went for 24hrs but PMA and FMLP went for 30 min. Thereafter, cell culture medium was aspirated, followed by the addition of 100µl of 1: 100 diluted Luciferin-NT and GST mixture in a reaction buffer for 30 min at RT (Anatech, RSA). This was then followed by the addition of equal volume of reconstituted Luciferin detection reagent for 15 min for the development of luminescence, then measurement was accomplished using using GloMax-Multi microplate reader (Promega, USA).

2.9 The evaluation of the effects of Lithium on expression level of several genes that are linked to nuclear factor kappa-light-chain-enhancer of activated B cells (NF-κB) signalling pathway

2.9.1 Total RNA Isolation from Raw 264.7 macrophage cells

Raw 264.7 cells were cultured in a 60 mm cell culture dishes for overnight at a density of 6 x 10^6 cells/ml. Thereafter, cells were treated with 10 mM LiCl, 10 µm/ml LPS, 10 µg/ml PMA and 10 µg/ml FMLP, as well as combination of 10 mM LiCl with each of the above mentioned stimulants. The treatment with 10 mM LiCl and LPS

went for 24 hrs, and then in the case of combination of the 10 mM LiCl, PMA and FMLP the salt was incubated for 24 hrs and stimulants for 30 min. RNeasy Mini Kit was used to isolate total RNA according to manufacturer's protocol (Qiagen, USA). Cells were harvested by scraping with a cell scraper and pelleted by centrifugation for 5 min at 300 x *g.* Cells were washed once with 1 x PBS and lysed with 400 µl of lysis buffer RLT, and then mixed by vortexing. Lysate were transferred into a QIAshredder spin column placed in a 2 ml collection tube, and centrifuged for 2 min at a 10 000 *x g*. One volume of 70 % ethanol was added to the lysate and mixed, and then 700 µl of mixture of lysate and ethanol was transferred to RNeasy spin column placed in a 2 ml collection tube. The mixture was centrifuged for 1 min at 800 x *g* at 25^{o}C, after centrifugation the flow through was discarded. Thereafter, 700 µl of buffer (RW1) was added in the RNeasy spin column, and centrifuged for 1 min at 800 x *g* at 25^{o}C*,* and the flow through was discarded. The 500 µl of buffer RPE was then added to RNeasy spin column and centrifuged for 1 min at 800 x *g* at 25^{o}C*,* and then flow through was discarded*.* RNeasy spin column was placed in a new 1.5 ml collection tube and then 50 µl of RNase-free water was added in the RNeasy spin column followed by centrifugation for 2 min at 8000 x *g* to elute the RNA. Thereafter, RNA was stored at - 80^{o}C for cDNA synthesis.

2.9.2 cDNA synthesis with RT^{2} Fist strand kit

The synthesis of cDNA was carried out with RT^{2} Fist strand kit according to manufacturer's protocol (Qiagen, USA). Ten microliters of genomic DNA elimination mixture which contains; 1 µg RNA, 2 µl buffer GE and RNase free-water that sum up to 10 µl. This mixture was incubated for 5 min at 42^{o}C then the reaction was stopped placing the mixture on ice for 1 min. Ten microliters of revers transcription mixture containing; 24 µl 5 x buffer BC3, 6 µl Control P2, 12 µl RE3 reverse transcriptase and 18 µl RNase-free water summing up to 60 µl was added in 10 µl of genomic DNA elimination mixture. This mixture was then incubated for 15 min at 42^{o}C, and then the reaction was stopped by incubation for 5 min at 95^{o}C. Afterwards, 91 µl of RNase free-water was added to the cDNA, and then followed cDNA stored at -80^{o}C.

2.9.3 Real time PCR

In order to analyse the gene expression in each sample a 96 well plates were used. A 1350 µl mixture of 2x RT^{2} SYBR Green Matermix, 102 µl cDNA synthesis reaction

and RNase-free water, which sums up to 2700 µl were mixed. Prior to addition of PCR components mixture, the 96-well arrays were briefly centrifuge at 300 x *g* for 2 min. Twenty five microliters of PCR components mixture was added to each well of RT^2 profiling PCR Arrays and the RT^2 profiling PCR Arrays were tightly sealed with optical thin-wall 8 strips and the arrays were briefly centrifuged at 1000 x *g* for 1 min at 25^oC. Thereafter, 40 cycles were accomplished 1 cycle for 10 min at 95^oC and 40 cycles of 15 s at 95^oC and 1 min at 60^oC.

Table 1.1: NFκB pathway gene table with accession numbers of the primer genes used in the Profiler Real Time PCR array assay in LPS activated Raw 264.7 macrophages.

NFκB Pathway associated gene	Description	Unigene	GeneBank
Tollip	Toll interacting protein	Mm.103551	NM_023764
Traf3	Tnf receptor-associated factor 3	Mm.27431	NM_011632
NFκBia/ IκB-α	Nuclear factor of kappa light polypeptide gene enhancer in B-cells inhibitor, alpha	Mm.170515	NM_010907
NFκB1/p50	Nuclear factor of kappa light polypeptide gene enhancer in B-cells 1, p105	Mm.256765	NM_008689
Traf2	Tnf receptor-associated factor 2	Mm.3399	NM_009422
Akt1	Thymoma viral proto-oncogene 1	Mm.6645	NM_009652
Bcl3	B-cell leukemia/lymphoma 3	Mm.439658	NM_033601
Ccl2	Chemokine (C-C motif) ligand 2	Mm.290320	NM_011333
Chuk	Conserved helix-loop-helix ubiquitous kinase	Mm.3996	NM_007700
Csf2	Colony stimulating factor 2 (granulocyte-macrophage)	Mm.4922	NM_009969
Csf3	Colony stimulating factor 3 (granulocyte)	Mm.1238	NM_009971
Ifng	Interferon gamma	Mm.240327	NM_008337
IκBkb	Inhibitor of kappaB kinase beta	Mm.277886	NM_010546
IκBke	Inhibitor of kappaB kinase epsilon	Mm.386783	NM_019777
		Mm.12967	NM_010547
Il10	Il10 Interleukin 10	Mm.874	NM_010548

Il1a	Interleukin 1 alpha	Mm.15534	NM_010554
Tnf	Tumor necrosis factor	Mm.1293	NM_013693
Il1b	Interleukin 1 beta	Mm.222830	NM_008361
IκBkg	Inhibitor of kappaB kinase gamma	Mm.12967	NM_010547
Map3k1	Mitogen-activated protein kinase kinase kinase 1	Mm.15918	NM_011945
Mapk3	Mitogen-activated protein kinase 3	Mm.8385	NM_011952
Myd88	Myeloid differentiation primary response gene 88	Mm.213003	NM_010851
NFκB2/p52	Nuclear factor of kappa light polypeptide gene enhancer in B-cells 2, p100	Mm.102365	NM_019408
Rela	V-rel reticuloendotheliosis viral oncogene homolog A (avian)	Mm.249966	NM_009045
Relb	Avian reticuloendotheliosis viral (v-rel) oncogene related B	Mm.1741	NM_009046
C-Rel	Reticuloendotheliosis oncogene	Mm.4869	NM_009044
Icam1	Intercellular adhesion molecule 1	Mm.435508	NM_010493
Irak1	Interleukin-1 receptor-associated kinase1	Mm.38241	NM_008363
Irak2	Interleukin-1 receptor-associated kinase2	Mm.152142	NM_172161
Gapdh	Glyceraldehyde-3-phosphate dehydrogenase	Mm.343110	NM_008084
Actb	Actin, Beta	Mm.328431	NM_007393

2.10 Immunocytochemistry

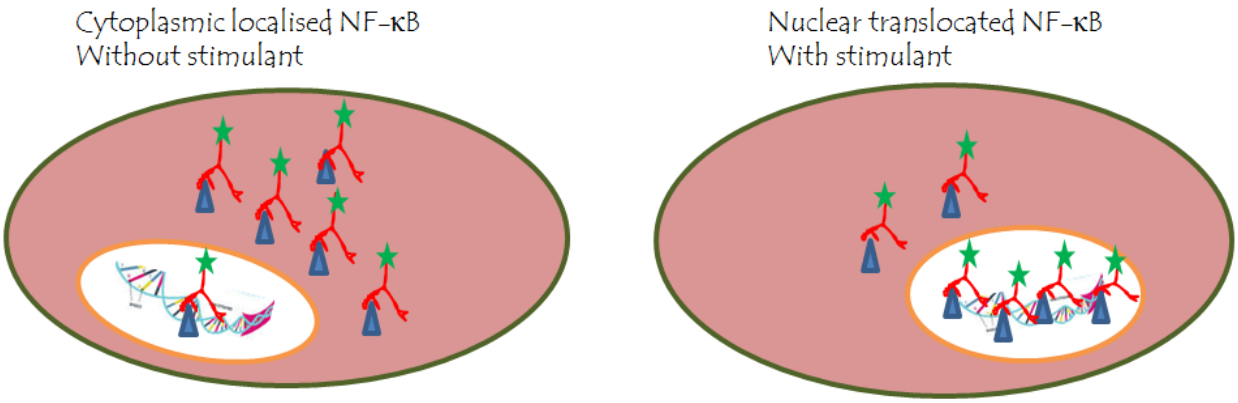

Figure 2.2: Demonstration of translocation of the NF-κB transcription factor from the cytoplasm to the nucleus. This figure demonstrates how to locate the translocated NF-κB transcription factor inside or outside the cell nucleus.This molecule is spotted by tracing the green fluorescent signal (shown by green stars) inside or outside the cell nucleus.

The translocation effects of lithium on NF-κB were assessed by immunofluorescence staining technique. Cells were cultured at a density of 6x 10^5 cells/ml on coverslips and allowed to adhere for 4 hrs. Thereafter, cells were treated with 10 mM LiCl, 10 mM NaCl, 100 ng/ml ultrapure LPS and combination of salts and LPS for 90 min. Cells were then washed with 1 x PBS and fixed at room temperature for 30 min with 3.7 % paraformaldehyde. Thereafter, cells were washed with 1 x PBS and permeabilised with permeabilising buffer [0.1 % Triton X-100, 1 % BSA in 1 x PBS] for 30 min. The nonspecific binding was blocked with 1 % BSA in 1 x PBS for an hour. Thereafter, cells were incubated with anti-NF-Kb antibody (1:500) for an hour, and then cells were washed 3 x with 1 x PBS, and stained for 30 min with anti-rabbit IgG-fluorescence (1:2000). After 30 min incubation, cells were washed with 1 x PBS and then followed DNA staining with 25 µg/ml Hoechst for 20 min at RT. Thereafter, coverslips were mounted on glass slides with mounting medium and then NF-κB translocation was analysed under fluorescence microscope (Nikon Eclipse TS100F, Japan).

2.11 Statistical analysis

Statistical analysis was performed in order to determine significant differences between samples. Differences were considered significant at,* $p<0.05$; ** $p<0.01$; *** $p<0.001$. The analysis of variants test (ANOVA), Tukey-Kramer was used to compare samples using Graph Pad Instat^{TM} 3 software. For Real Time PCR (gene expression studies) Quagen data analysis website and housekeeping genes (Gapdh and β-Actin) C_t values where used to calculate the fold change of gene expression.

CHAPTER THREE

RESULTS

3.1 Effects of Lithium on the morphology, adhesion, growth and viability of Raw 264.7 and NIH 3T3 cells

Lithium was shown to be non-cytotoxic to both Raw 264.7 and fibroblast NIH 3T3 cell lines at concentrations between 0.3125 and 20 mM. Figures 3.1-3.3, illustrate that lithium, up to 20 mM, is non-cytotoxic in contrast to high concentrations of LiCl (50–100 mM LiCl) as demonstrated by MTT assay and xCelligence real time cell analyser system (RTCA). Moreover, Raw 264.7 cells retained their morphology after treatment with lithium concentrations ranging between 0.3125 and 20 mM (figure 3.1B). Treatment of NIH 3T3 cells with 10 mM lithium chloride resulted in no changes in cell viability, growth and morphology as compared to the control (0.02 mg/ml actinomycin-D) (figure 3.2). The current based xCELLigence (RTCA), as well showed that 1.25 - 20 mM lithium chloride is non-cytotoxic to Raw 264.7 cells, while 50-100 mM of lithium chloride was toxic more or less similar to control 0.02mg/ml actinomycin-D (figure 3.3).

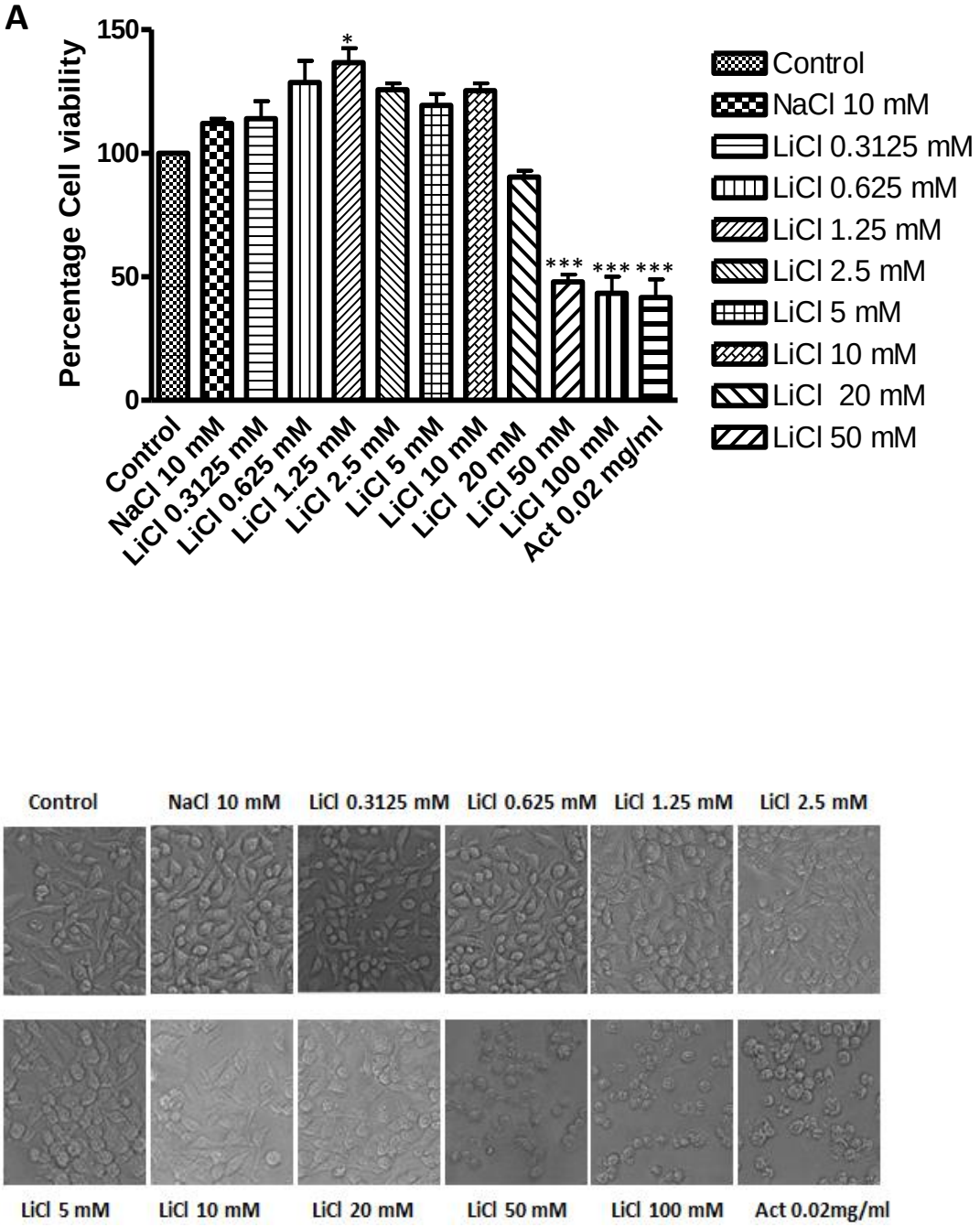

Figure 3.1: The effects of lithium on the viability and morphology of Raw 264.7 macrophage cells. Cells ($6x10^6$cells/ml) were seeded in 96-well and treated with various concentrations of LiCl, NaCl (10mM) and actinomycin-D (0.02 mg/ml) for 24 hrs. After 24 hrs of treatment images were captured under the Nikon Ti-E inverted microscope [B]. There after MTT was used to measure viability with GloMax-Multi microplate reader at 570 nm (Promega, USA)[A].

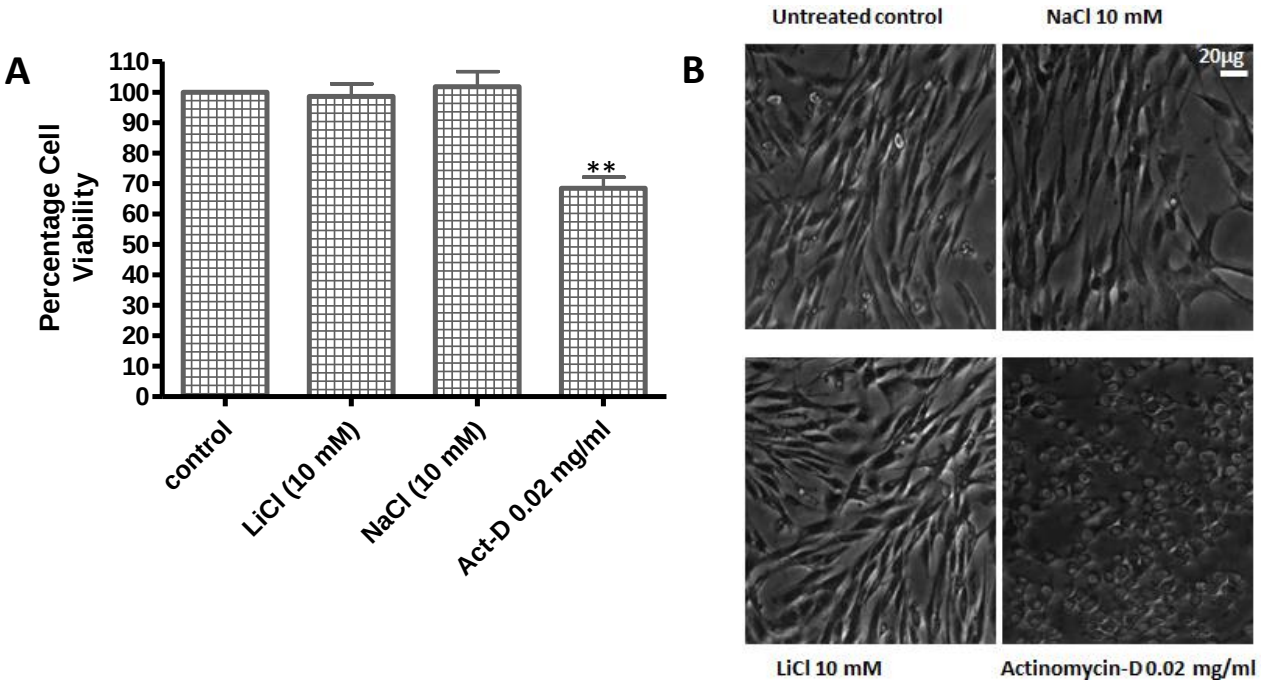

Figure 3.2: The effect of lithium on the morphology and viability of NIH 3T3 fibroblast cells. Cells were cultured in 96 well platse at a density of 6 x10^6 cells/ml and then treated with LiCi (10 mM), NaCl (10 mM) and actinomycin-D (0.02 mg/ml) for 24 hrs. Thereafter pictures wree captured with Nikon Ti-E inverted microscope and then cell viability was assessed using the MTT assay.

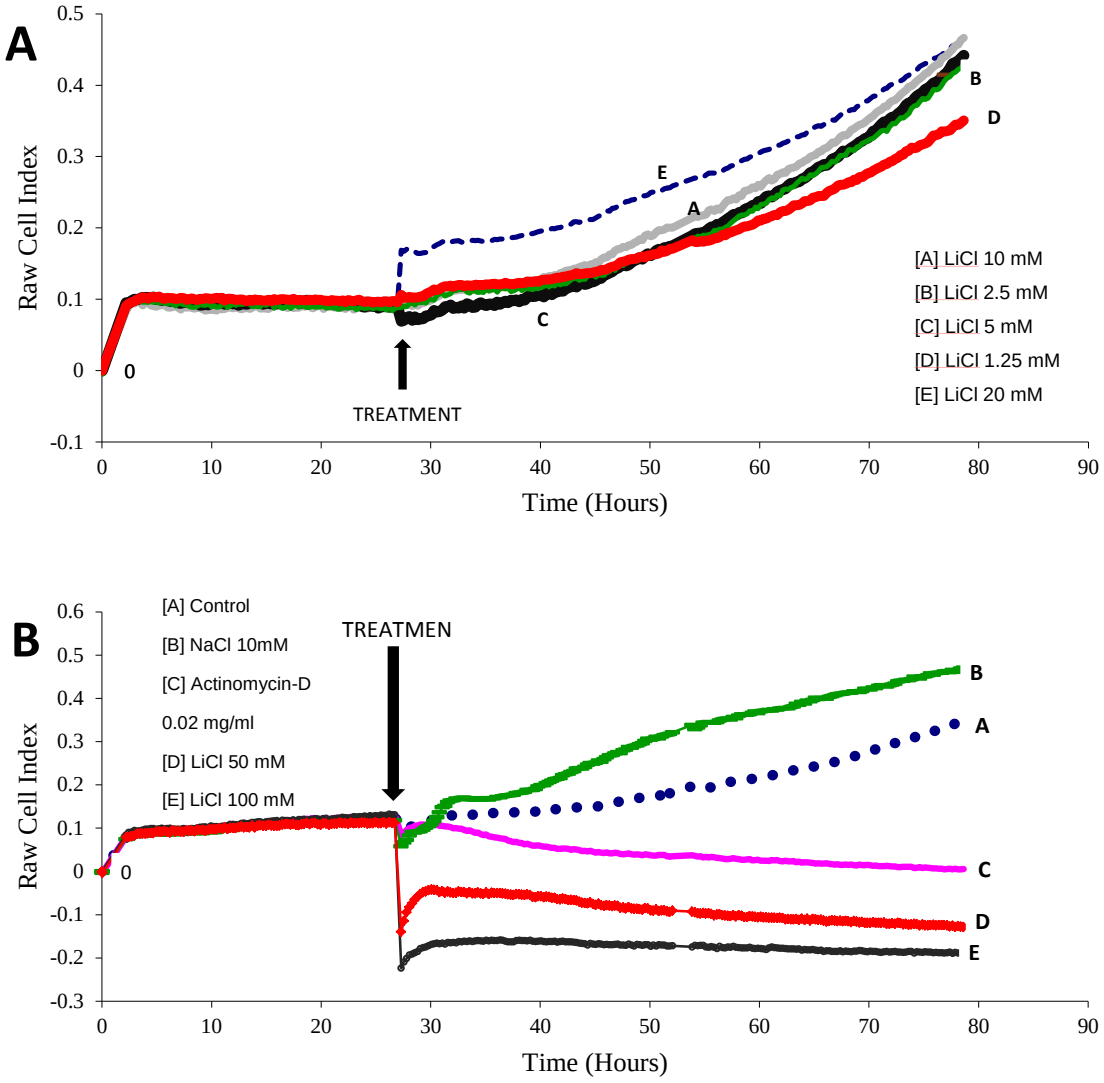

Figure 3.3: Determination of proliferative role of lithium on Raw 264.7 macrophage cells. Raw 264.7 cells were seeded at 40 000 cells/well in a microelectrical plate for 24 hrs, and then treated with 0.02 mg/ml actinomycin-D, 10 mM NaCl and various concentration of LiCl (100, 50, 20, 10, 5, 2.5, 1.25mM) for 56 hrs. This system measures electrical impedance as cell index that is determined by cell morphology, cell adhesion and cell number.

3.2 Apoptotic effects of lithium on Raw 264.7 and NIH 3T3 cells

Annexin-V and PI apoptosis detection assay is used to confirm the safety of lithium and or analysis of any apoptotic singes. The apoptosis detection was accomplished by the use of both the flow cytometry and Fluorescent microscopy. Fluorescent microscopy results showed that 10 mM LiCl does not induce apoptosis in Raw 264.7 cells. Cells treated with 10 mM lithium chloride retained their morphology and stained negative for both Annexin-V and PI. On the other hand cells treated with 0.02mg/ml actinomycin-D, lost their spindled shape morphology and stained positive for Annexin-V, but negative for PI (results not shown) (fig 3.4). NIH 3T3 cells treated with 10 mM lithium chloride also stained negative for Annexin-V and PI. However, 0.02mg/ml actinomycin-D treated cell stained positive for both Annexin-V and PI (figure 3.5).

In addition to microscopic analysis, flow cytometer as well shows that 5 -20 mM LiCl did not induce apoptosis in Raw 264.7 cells (fig 3.6). The flow cytometer plot is divided in to four quadrats, top left (Necrosis), top right (late phase of apoptosis), bottom left (viability/ normal cells) and bottom right (early phase of apoptosis). Untreated control, 10 mM NaCl and the cells treated with 5 mM LiCl,10 mM LiCl and 20 mM LiCl have a high cell count in the Annexin-V negative quadrant (bottom left) as shown by quadrant statistics (92.82%, 83.65%, 85.49% and 92.53%) respectively. In contrast 50 mM LiCl has a high cell count of 65.8 % in the Annexin-V positive quadrant (bottom right) and 11.38% of the cell count in the Annexin-V and PI positive quadrant (top right). However, control actinomycin-D (0.01 and 0.02 mg/ml) treatment has a major cell count in the top right quadrant (38.25% and 39.35%) and minor cells counts in the bottom right quadrant (20.16% and 15.51%).

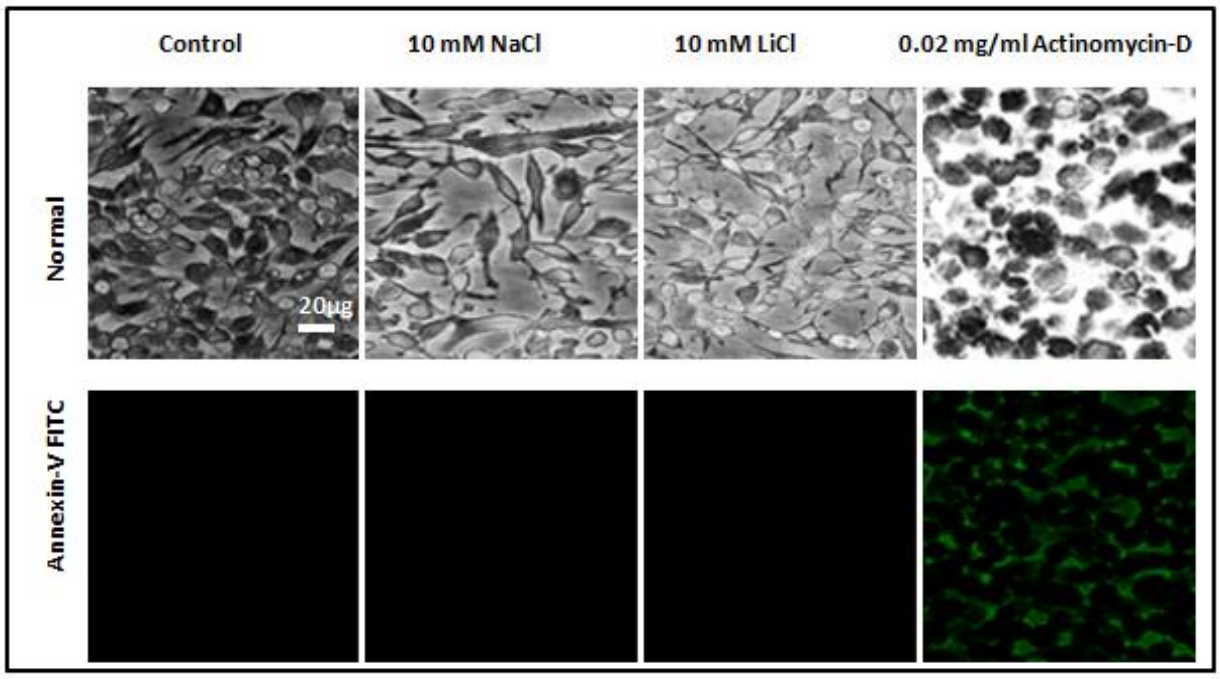

FIGURE 3.4: Determination of the apoptotic effect of lithium on Raw 264.7 macrophage cells. Cells were cultured at density of 6x10 ^{5} cells/ml, on coverslip in micropetri-dish. Followed by treatment of cell with 10 mM LiCl, 10 mM NaCl, 0.02 mg/ml actinomycin D for 24hrs. After 24 hrs, cells were staining with Annexin- V / PI for 20 min. Pictures were then captured at 20x magnification with Nikon Ti-E inverted microscope (Nikon, Japan).

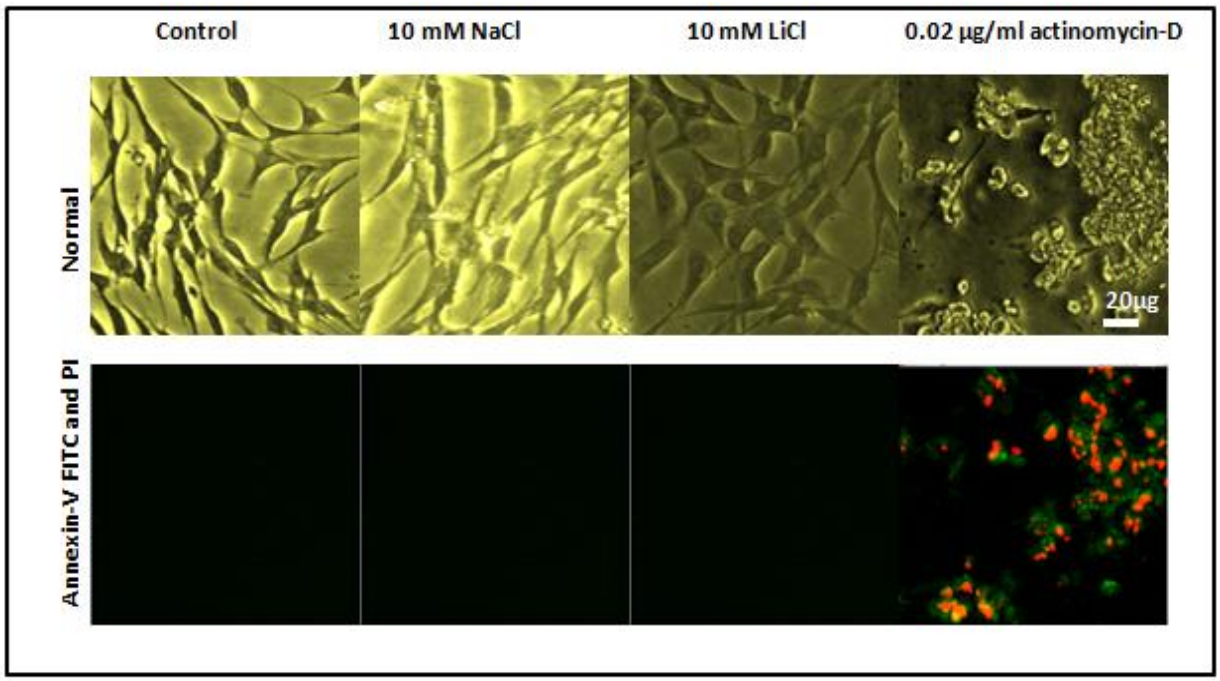

Figure 3.5: Determination of the apoptotic effect of lithium on NIH 3T3 fibroblast cells. Cells were seeded at $6x10^6$cells/ml on the cover slips, and treated with 10 mM LiCl, 10 mM NaCl, actinomycin-D 20 µg/ml for 24 hrs. The cells were then stained for 20 min with Annexin-V and PI. Fluorescence intensity was analysed with Nikon Ti-E inverted microscope at 20x magnification (Nikon, Japan).

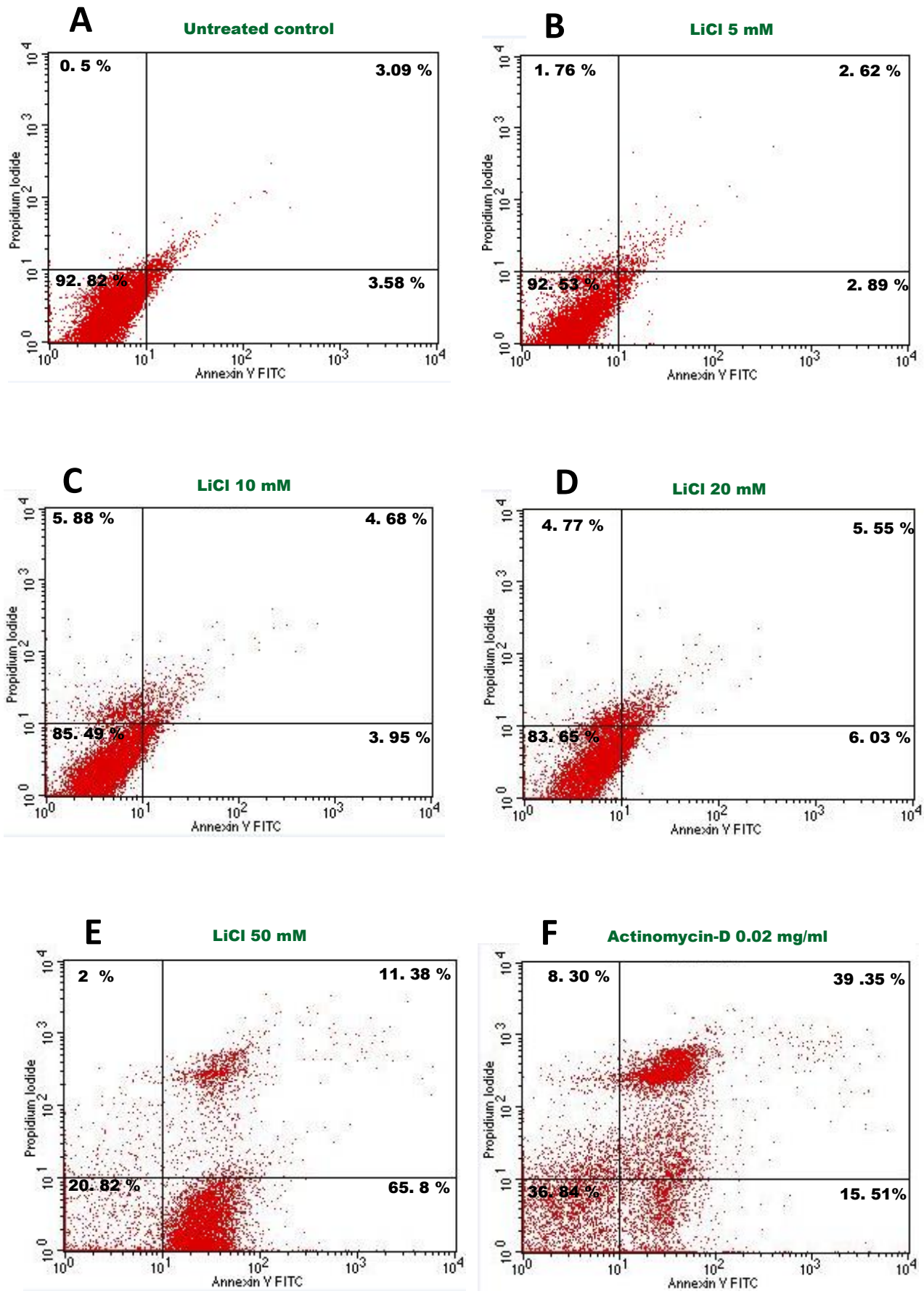
A
Untreated control
0. 5 %
3.09 %
92. 82 %
3.58 %
B
LiCl 5 mM
1. 76 %
2. 62 %
92. 53 %
2. 89 %
C
LiCl 10 mM
5. 88 %
4. 68 %
85. 49 %
3. 95 %
D
LiCl 20 mM
4. 77 %
5. 55 %
83. 65 %
6. 03 %
E
LiCl 50 mM
2 %
11. 38 %
20. 82 %
65. 8 %
F
Actinomycin-D 0.02 mg/ml
8. 30 %
39 .35 %
36. 84 %
15. 51%
Propidium Iodide
Annexin V FITC

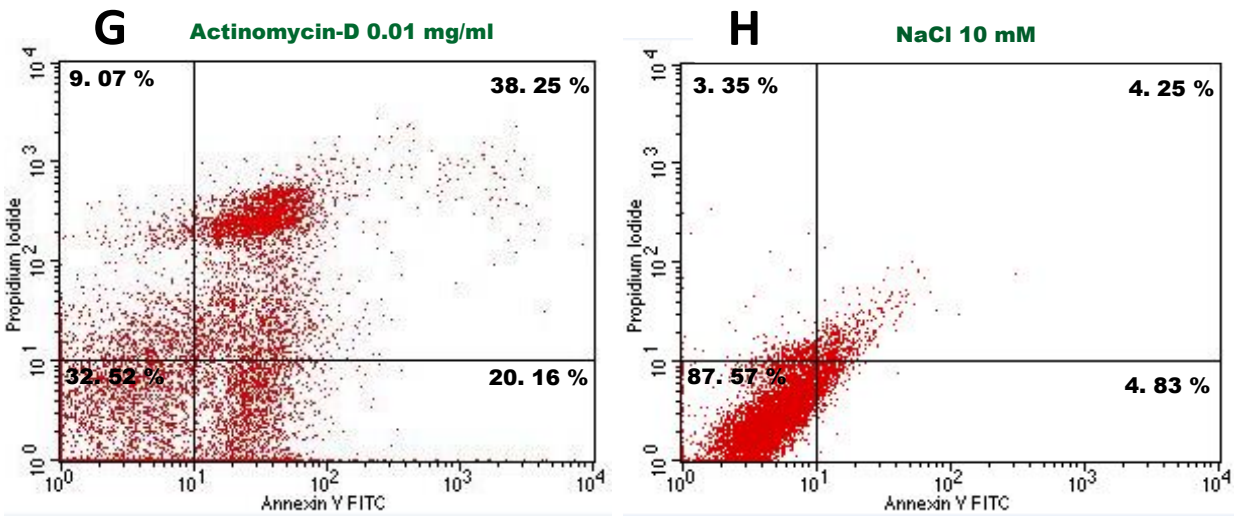

Figure 3.6: Apoptotic effects of lithium on Raw 264.7 macrophage cells using flow cytometry. Cells were seeded in a 200 mm dish at a density of $6X10^6$ cells/ ml. This was then followed by treating the cells with LiCl 5, 10, 20 and 50 mM LiCl, 10 mM NaCl as well as 0.01 and 0.02 mg/ml actinomycin-D for 24 hrs. Cells where thereafter stained with Annexin-V/ PI for 20 min in the dark, and then cell analysis was carried using flow cytometer (BD-Biosciences, USA) according to manufacturer's protocol.

3.3 Effects of lithium on LPS-induced Nitric Oxide production in Raw 264.7 cells

The results showed that lithium at doses levels less than than 10 mM reduces NO production (fig 3.7). Cells treated with both Lithium chloride (1.25, 2.5 and 5 mM) and 10 µg/ml LPS produce less nitric oxide as the non-stimulated LiCl salt. In contrast, the untreated control varied significantly with LPS stimulated cells in NO production ($p<0.05$), similar variation occurred in 10 mM NaCl and 10 mM LiCl when compared to their combination treatment that encompasses the above mentioned salts and LPS stimulant (fig 3.7)

Effects of lithium on the production of NO were further assessed with a cell permeate Nitric oxide indicator DAF2-DA. The results of this assay also showed that low concentrations of 5 mM LiCl reduces NO production. Low fluorescence intensity was observed in the cells treated with 5 mM lithium chloride coupled 100 ng/ml ultrapure LPS treated cells as compared to 100 ng/ml ultrapure LPS (fig 3.8). Moreover, no

difference in NO production was observed between 5 mM lithium chloride and 5 mM lithium chloride coupled 100 ng/ml ultrapure LPS.

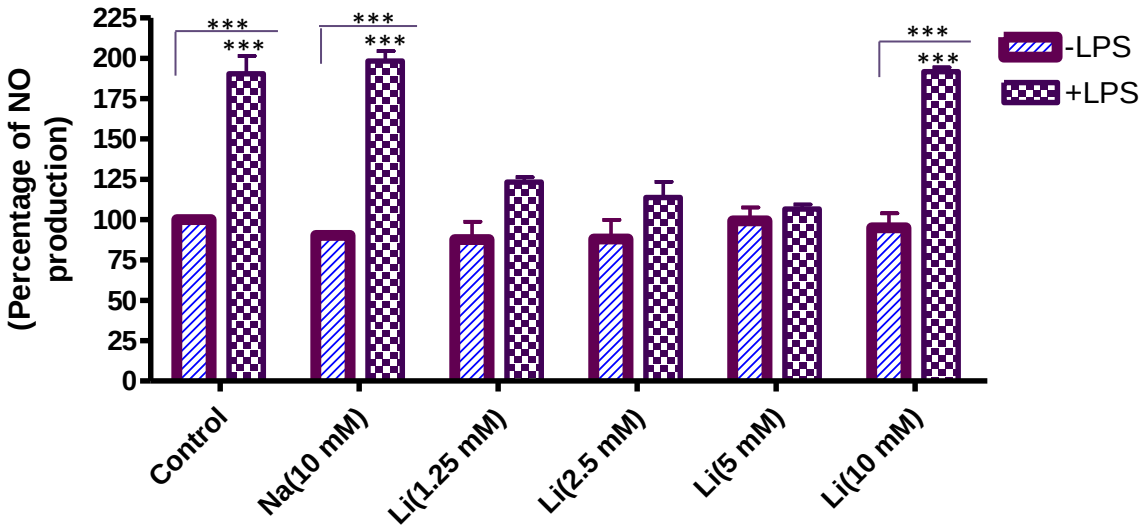

Figure 3.7: The Effect of lithium on Nitric oxide (NO) production assessed using Griess reagent in LPS stimulated Raw 264.7 cells. Cells were seeded at a density of $6x10^6$ cells /ml and treatment was executed by pre-treating with 10 mM NaCl and LiCl (1.25, 2.5, 5 and 10 mM) for an hour thereafter, other set of wells contained combinatory treatment that include 10 µg/ml LPS and the above mentioned salts for 24 hrs. Quantitation of nitric oxide production was carried out with Griess reagent at 550 nm using (Promega, USA).

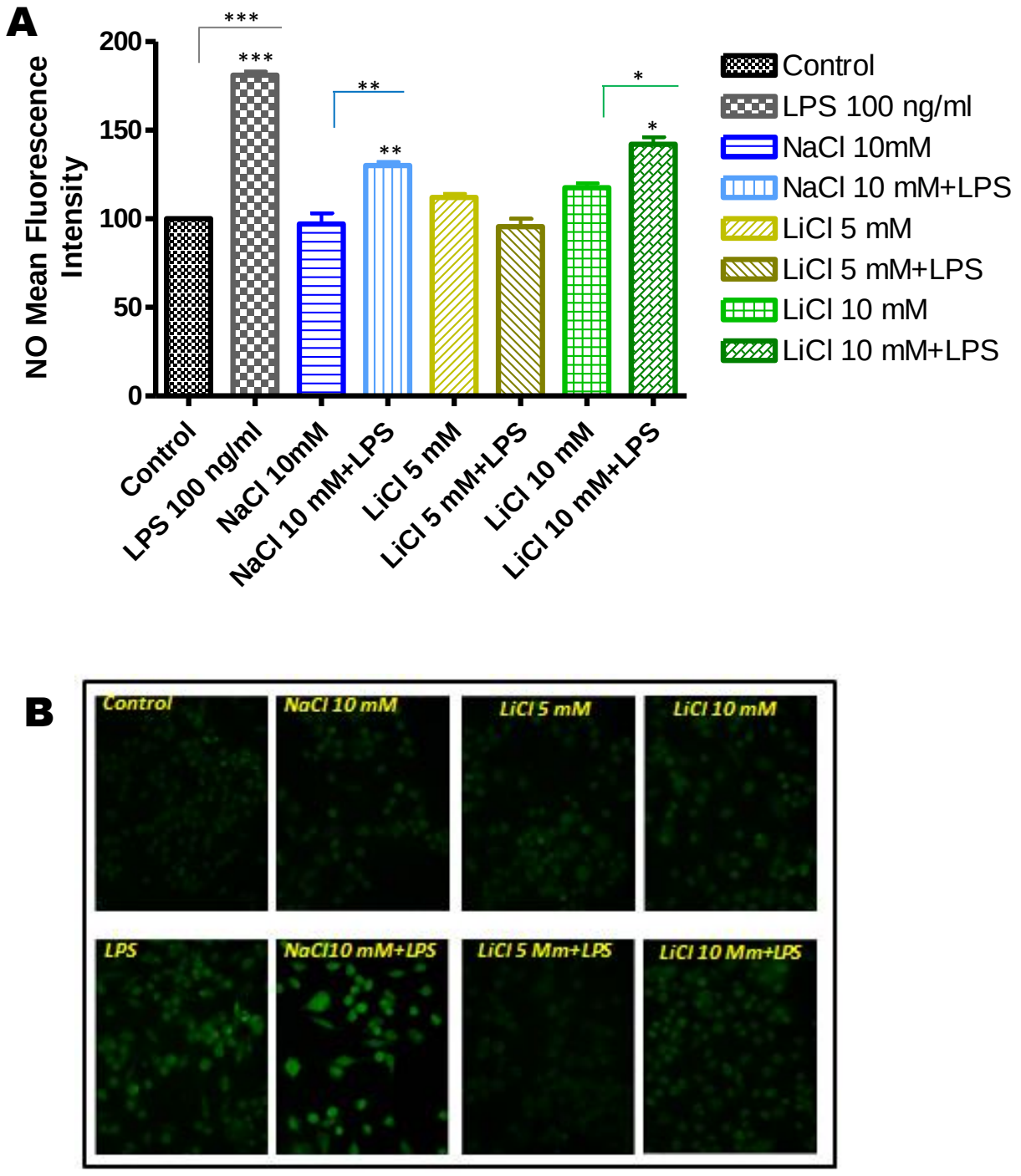

Figure 3.8: Determination of effect of lithium on nitric oxide production in LPS induced Raw 264.7 cells. Cells were seeded ($6x10^6$ cell/ml) and treated with LiCl (5 and 10 mM), 10 mM NaCl, 100 ng/ml LPS, combination of each of the chemicals with LPS for 24 hrs. Cells were stained with DAF2-DA for 20 min at RT in the darck. The measurement of the fluorescence was accomplished with Nikon Ti-E inverted microscope [B]. NIS Element view imaging software was used to measure fluorescence intensity (NIKON, JAPAN)[A].

3.4 Lithium inhibits oxidative burst as stimulated by LPS on Raw 264.7 macrophages

Figure 3.9 shows that 10 mM lithium chloride altered ROS production, as evidenced by changed fluorescence intensity. The stimulated Raw 264.7 cells showed high fluorescence intensity as compared to the cells treated with both the stimulant and 10 mM lithium chloride. This variation in fluorescence intensity was as well shown by measurement of fluorescence intensity using the NIS Element view imaging software (NIKON, Japan) (fig 3.9 B). There is significant difference in fluorescence intensity between cells treated with LPS and the combination of 10 mM lithium chloride and LPS.

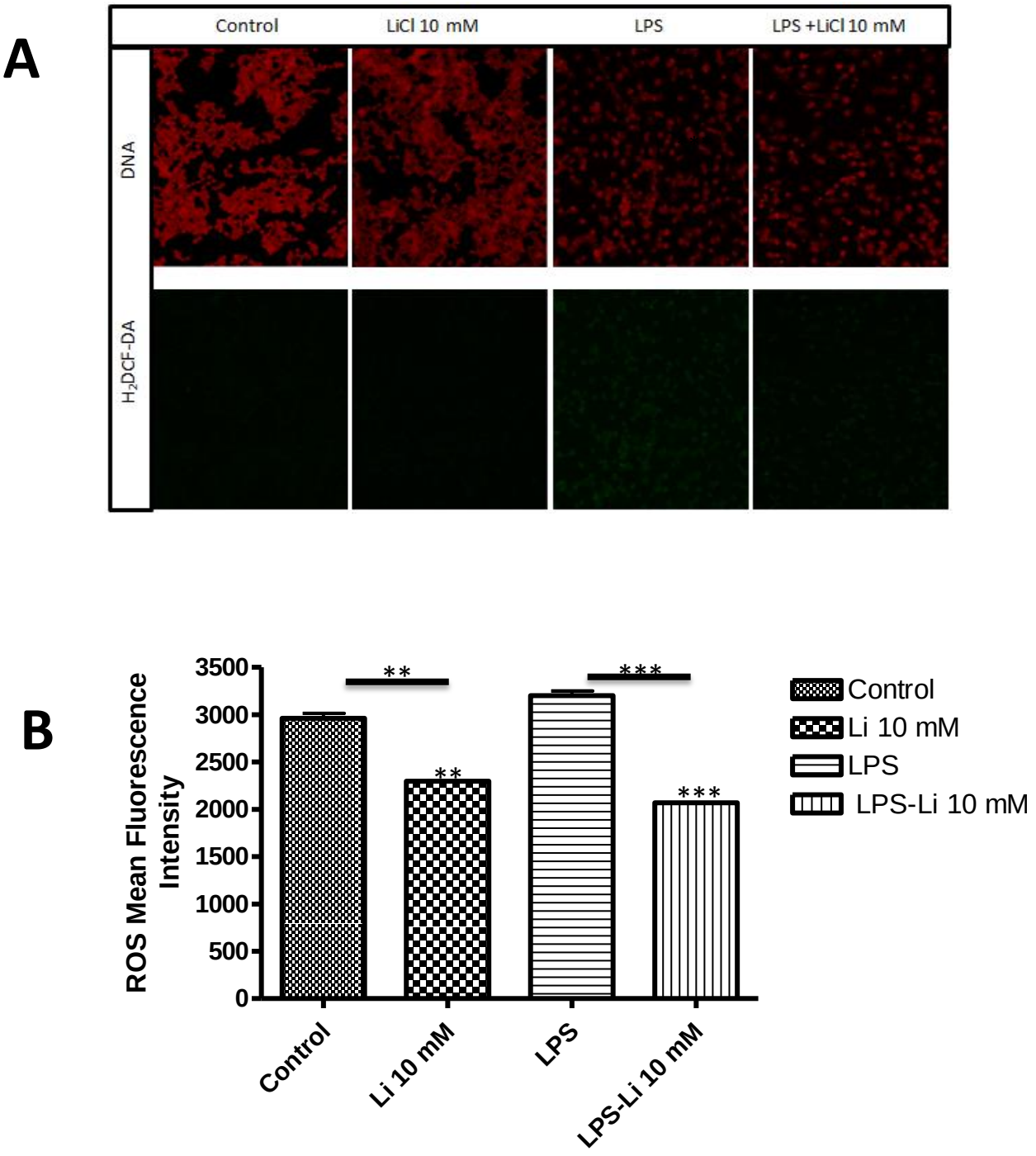

FIGURE 3.9: Effect of lithium on oxidative burst stimulated by LPS on Raw 264.7 macrophage cells. Raw 264.7 macrophage cells were seeded at a density of $6x10^5$ cells/ml on a cover slip. Cells were pre-treated with 10 mM LiCl prior treated with 10 µg/ml LPS for 24 hrs. The fluorescence was measured with Nikon Ti-E inverted microscope [A]. Fluorescence intensity of the pictures was measured using the NIS Element view imaging software (NIKON, JAPAN) [A].

3.5 Effects of lithium on production of glutathione by Raw 264.7 macrophages after LPS stimulation

The presence of glutathion was measured through conversion of a luciferin derivative into luminescent luciferin in the presence of glutathione, catalysed by glutathione S-transferase (GST). Figure 3.10 showed that 10 mM lithium chloride significantly enhanced the production of GSH. However, the treatment of lithium and LPS showed a lower amount of GSH as compared to lithium chloride treated cells. These results suggest that lithium might be lowering production of ROS through stimulation of GSH.

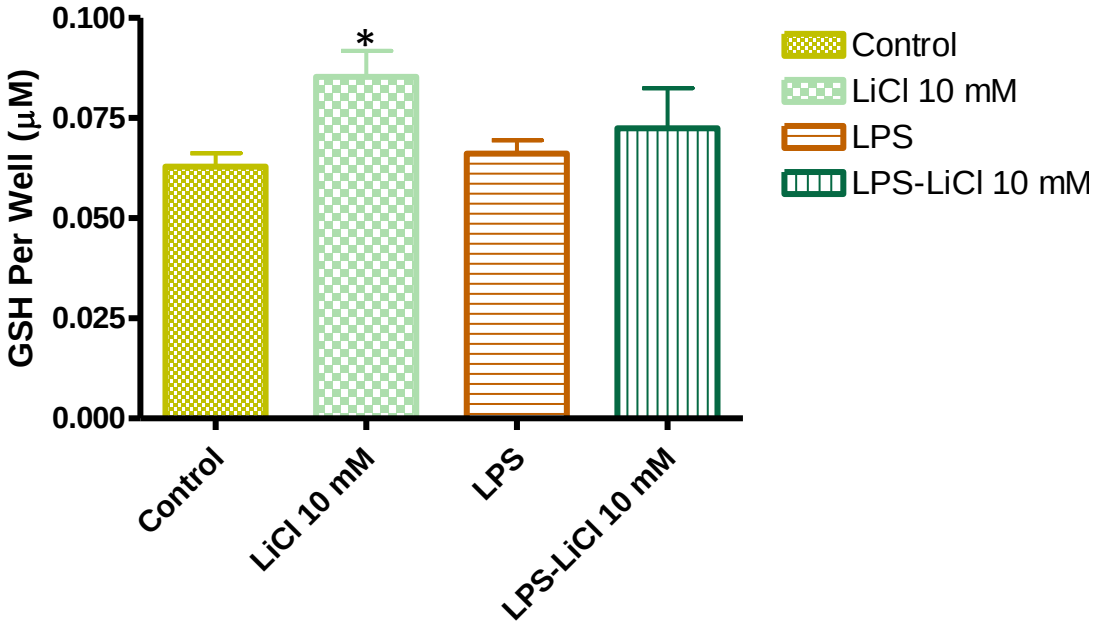

Figure 3.10: Evaluation of effects of lithium on production of Glutathione on LPS stimulated Raw 264.7 macrophages. Raw 264.7 cells were culture at a density of 10 000 cells/ml and treated with 10 mM LiCl, 10 mM NaCl and 100 ng/ml ultrapure LPS and combination of the salts and LPS for 24 hrs. Measurement of GSH was accomplished by GSH-Glo glutathione assay according to manufacturer's protocol. Thereafter, the produced luminescence was measured with GloMax-Multi microplate system (Promega, USA).

3.6 Effects of lithium on the translocation of NF-κB transcription factor after LPS stimulation

To study effects of lithium on the translocation of NF-κB after stimulation with LPS, immunocytochemistry was used. Figure 3.11 depicts that lithium chloride reversed the translocation of the NF-κB as compared to untreated control and 100 ng/ml LPS stimulated cells. In the untreated control NF-κB was observed in the cytosol as indicated by cells having uniform green fluorescence on the outskirts of the cell. In contrast, NF-κB was observed in the nucleus in LPS stimulates cells as evidenced by the intense green fluorescence with in the nucleus. In the overlay pictures the nucleus dye (Hoechst) is not as intense as in the control since, there is a mixture of blue and green. Moreover, exposure of 10 mM LiCl showed a decrease or reverse in NF-κB nuclear translocation, since the signal is spread all over the cell (in the cytoplasm and nucleus).

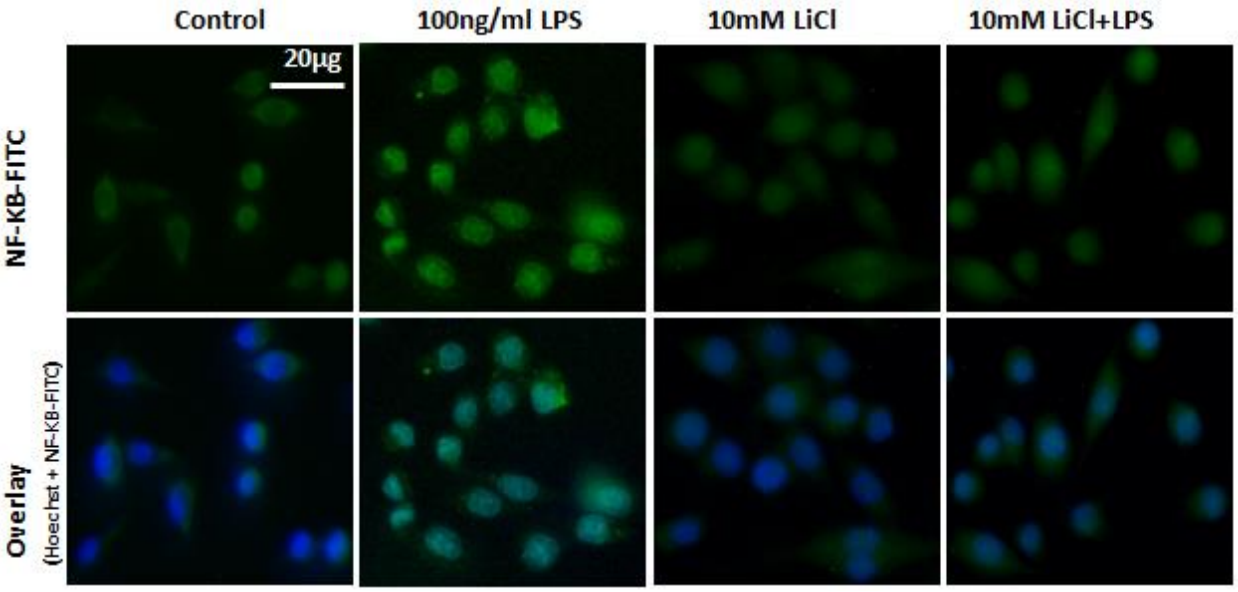

Figure 3.11: Evaluation of effects of lithium on nuclear translocation of NF-κB after LPS stimulation of Raw 264.7 cells. Raw264.7 cells were cultured at a density of x10^5 cells/ml on coverslips and allowed to adhere for 4hrs. Thereafter, cells were treated with 10 mM LiCl, 10 mM NaCl, 100 ng/ml ultrapure LPS and combination of salts and LPS for 90 min. Thereafter, anti-NF-κB antibody (1:500) was added for an hour, and then anti-rabbit IgG-(FITC) (1:2000) followed for an hour as well. Staining with 25 µg/ml Hoechst followed for 20 min, and then pictures were captured with inverted fluorescence microscope (Nikon Eclipse TS100F, Japan).

3.7 Effects of lithium on the expression profiles of NF-κB signalling related genes in LPS stimulated Raw 264.7 cells.

Real Time PCR (profiler array) was used to determine the effects of lithium on the expression profiles of genes involved in NF-κB signalling pathway. Dot plot was developed using C_t values from qiagen web based data analysis comparing control with combinatory treatment of 10 mM LiCl and LPS. This plot gives an overview of the expression criteria of the analysed genes (fig 3.12). The results showed an increase in the expression levels p50 subunit in the cells exposed to a combination of LPS and 10 mM LiCl as opposed to cells treated with 10 mM LiCl or LPS (fig 3.13 A). IκB-α expression was as well elevated in the cells treated with both LPS and 10 mM LiCl. (fig 3.13 B). Tollip and Traf3 proteins expression levels were increased after treatment with 10 mM LiCl and combinatory treatment (LPS and 10 mM LiCl) (fig 3.13 C). Figure 3.13 D, showed an increased expression of IL1-A, IL1-B, TNF-α and CSF3 in LPS and combinatory (LPS and 10 mM LiCl) treatment. However, CSF3 showed to be overexpressed as compared to the above mentioned genes.

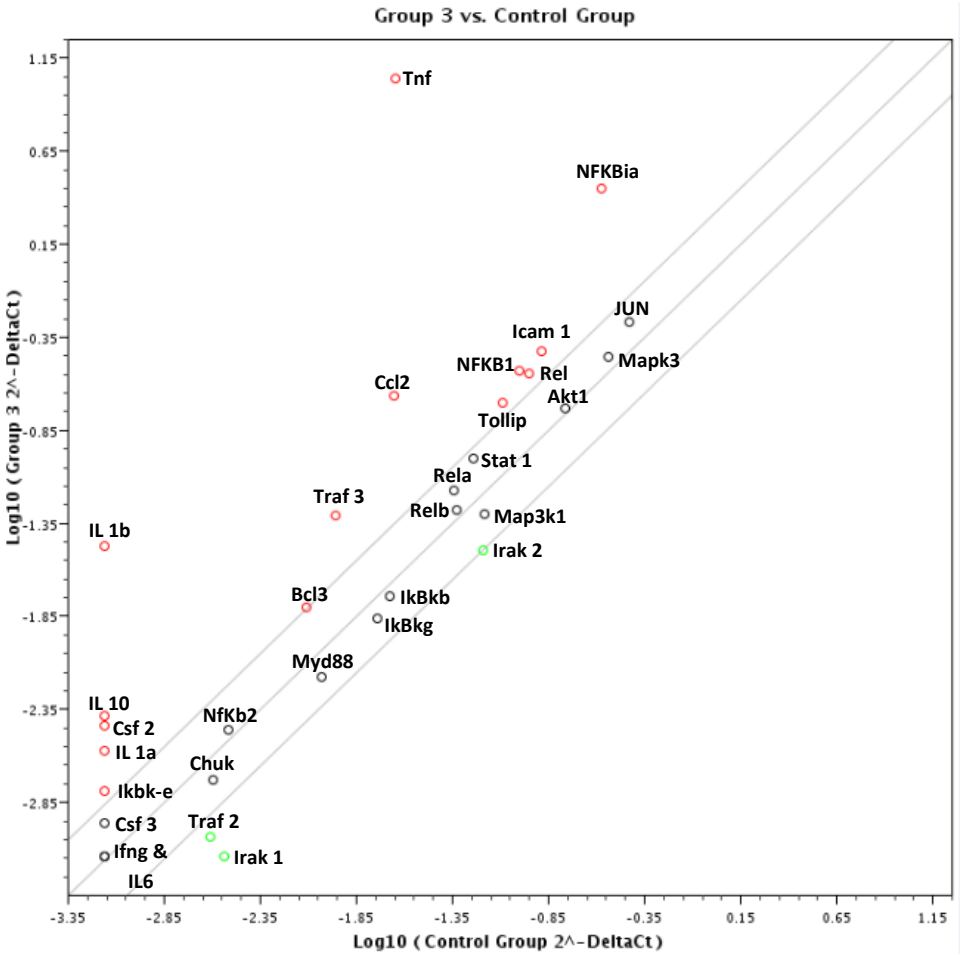

Figure 3.12: Expression of the NF-κB signalling related genes as shown by the Dot plot. In order to examine the expression profiles which lithium possesses, cells were cultures at a density of of $6X10^6$ cell/ ml in a 60 mm cell culture dishes. After Total RNA was isolation with Qiagen Total RNA isolation kit and then cDNA was synthesised with RT^2 Fist strand kit. The micro array were used to measure the expression profiles where 40 cycles where accomplished. The dot plot was developed with the C_t values using the Qiagen data analysis website.

A

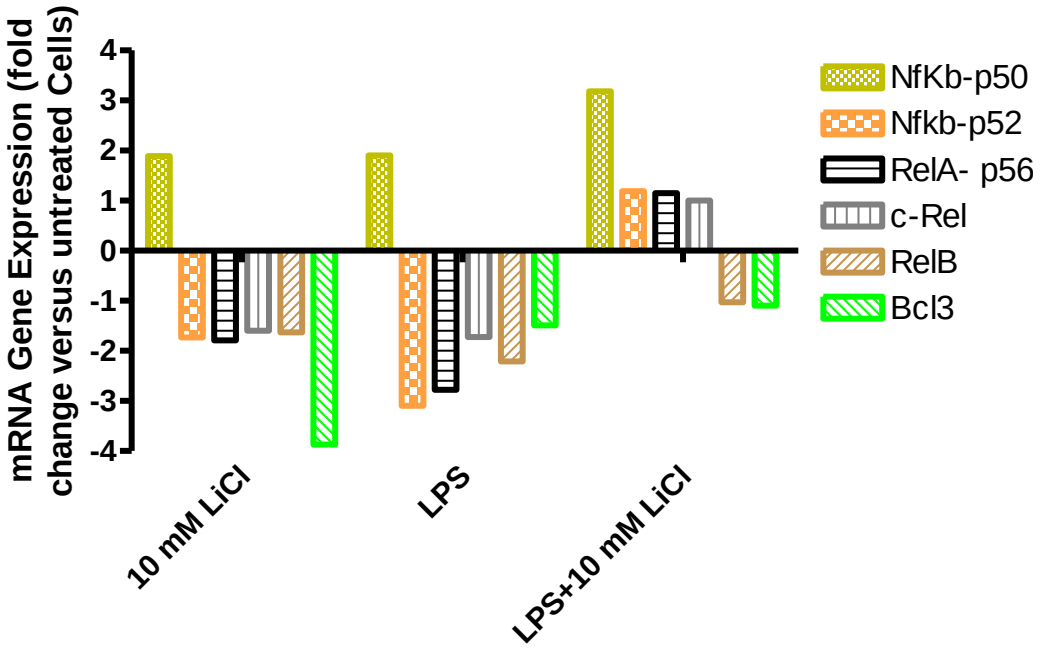
mRNA Gene Expression (fold change versus untreated Cells)
4
3
2
1
0
-1
-2
-3
-4
10 mM LiCl
LPS
LPS+10 mM LiCl
NfKb-p50
Nfkb-p52
RelA- p56
c-Rel
RelB
Bcl3

B

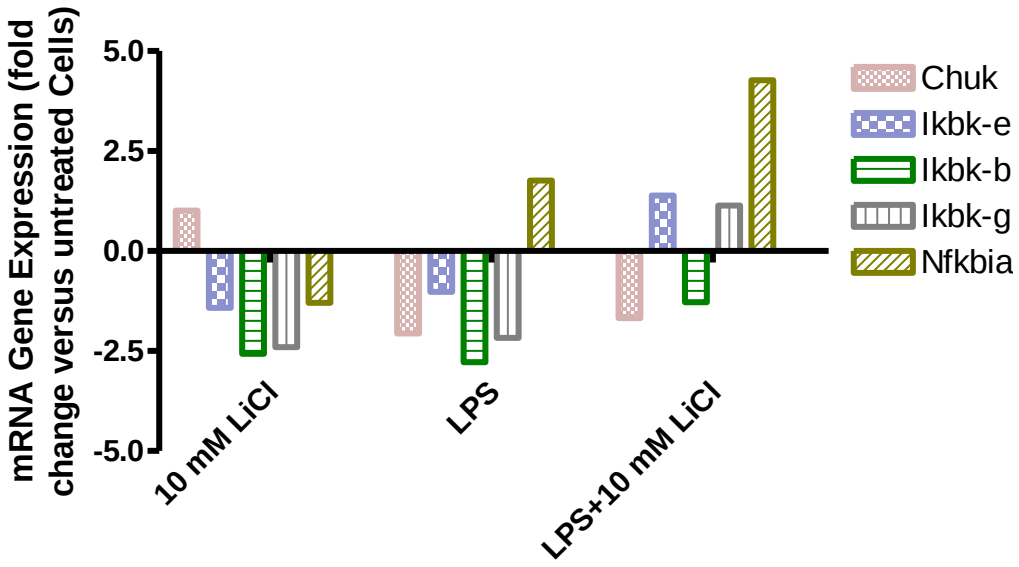
mRNA Gene Expression (fold change versus untreated Cells)
5.0
2.5
0.0
-2.5
-5.0
10 mM LiCl
LPS
LPS+10 mM LiCl
Chuk
Ikbk-e
Ikbk-b
Ikbk-g
Nfkbia

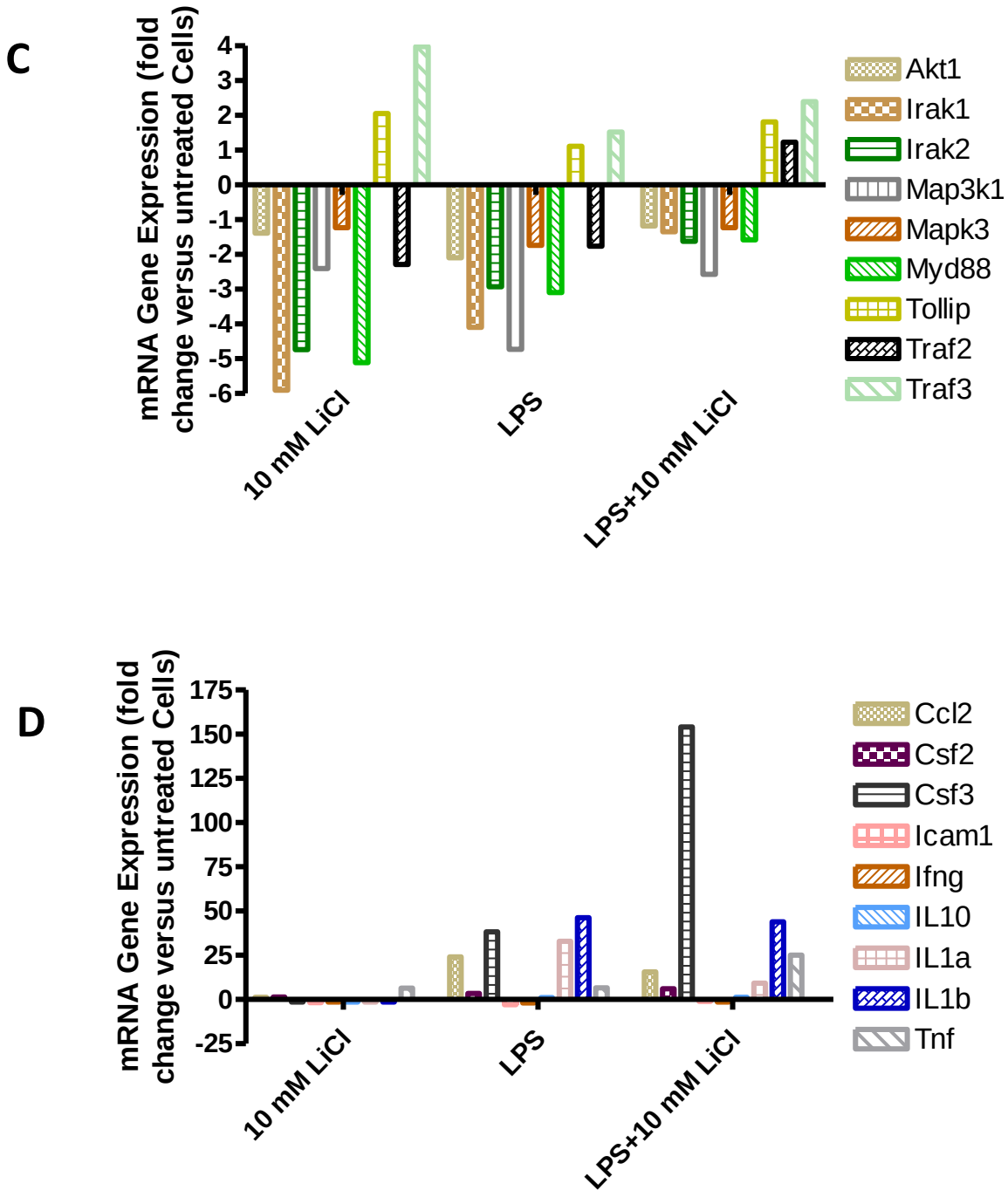

Figure 3.13: The effects of lithium on the expression of NF-κB signalling related genes on Raw 264.7 macrophages activated by LPS. Raw 264.7 cells were cultured in a 60 mm cell culture dishes overnight at a density of $6x10^6$ cell/ml. Thereafter, cells were treated with 10mM LiCl, 10 µm/ml LPS as well as combination of the lithium with LPS for 24hrs. RT^2 profiling PCR Arrays were used to measure the expression profiles of NF-κB were in which 40 cycles where accomplished.

Thereafter, Qiagen web based data analysis, was used to analyse the C_t values and then graph pad prism was used to plot the graphs.

3.8 Lithium inhibits oxidative burst as stimulated by PMA on Raw 264.7 cells

The oxidative burst was further measured using PMA as the stimulant, the assay was used as outlined in the materials and methods. The results revealed that treatment of Raw 264.7 cells with 10 mM Lithium chloride lowers ROS production, as seen by decreased fluorescence intensity (fig 3.14). The PMA stimulated Raw 264.7 cells had significant high fluorescence intensity as compared to PMA stimulated cells that were treated with 10 mM lithium chloride.

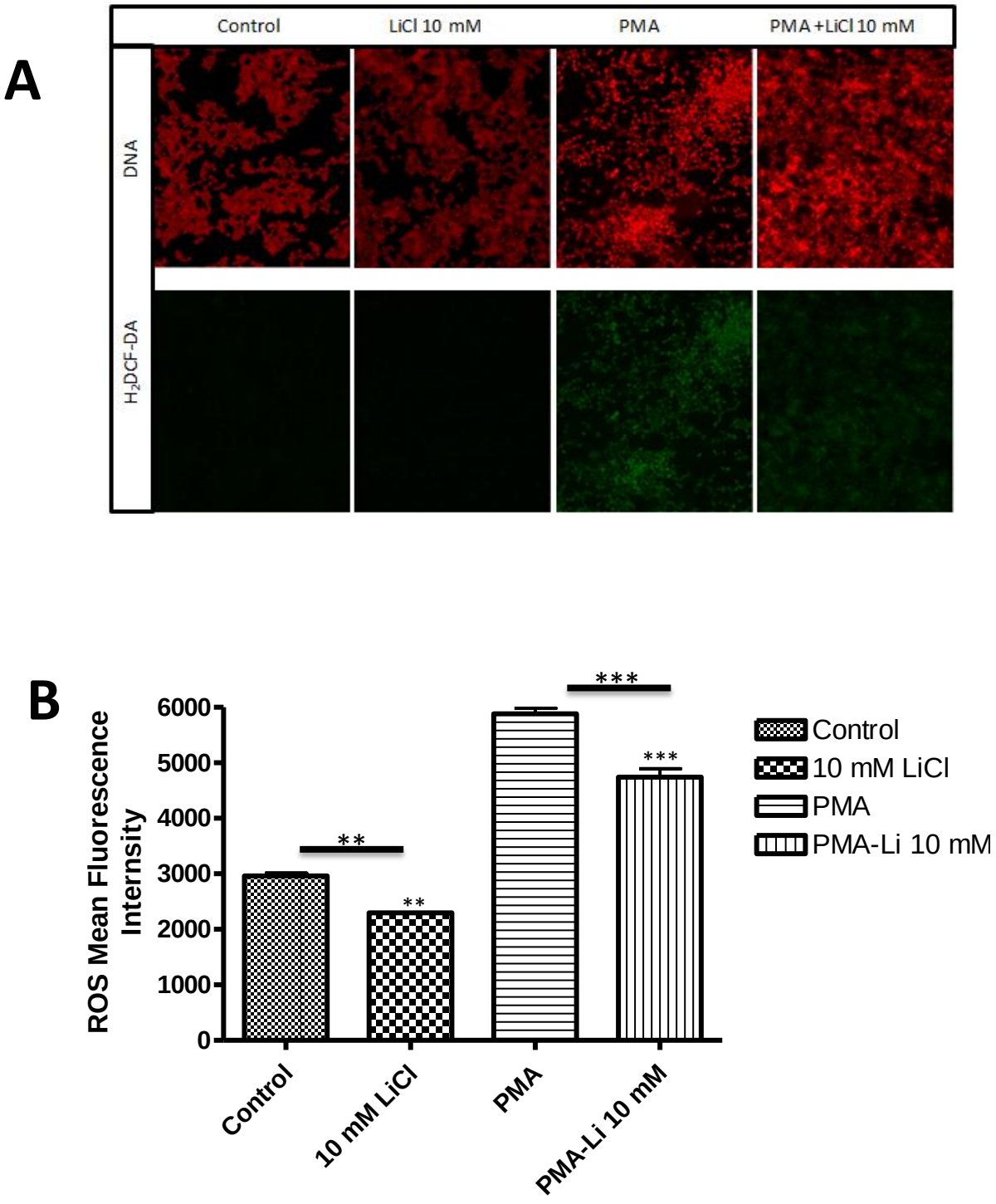

FIGURE 3.14: Effect of lithium on oxidative burst stimulated by PMA on Raw 264.7 macrophage cells. Raw 264.7 macrophage cells were seeded at a density of $6x10^5$ cells/ml on a cover slip. Cells were pre-treated with 10 mM LiCl for 24 hrs and stimulation with 10 ng/ml PMA for 30 min. The cell imaging was executed with the use Nikon Ti-E inverted microscope [A]. Fluorescent intensity was measured using the NIS Element view imaging software (NIKON, JAPAN). The plot was done using Graph pad prism-4 software [B].

3.9 Effects of lithium on production of Glutathione by Raw 264.7 macrophages after PMA activation

In order to gain an insight on the anti-inflammatory role of lithium chloride, GSH molecule was measured through conversion of a luciferin derivative into luminescent luciferin in the presence of glutathione, catalyzed by glutathione S-transferase (GST). Treatment with lithium chloride elicited a significant variation in production of GSH. The cells that are PMA-stimulated have low GSH as compared to cells that are both PMA-stimulated and treated with 10 mM LiCl.

.

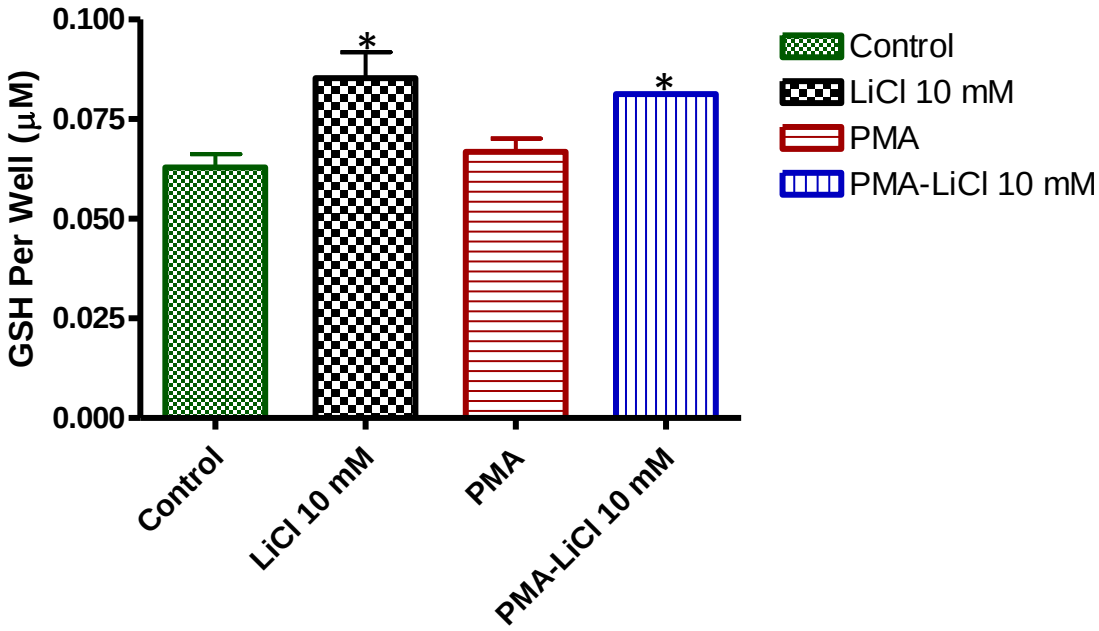

Figure 3.15: Evaluation of effects of lithium on production of Glutathione on PMA stimulated Raw 264.7 macrophages. Raw 264.7 cell were culture at a density of 10 000 cells/ml overnight. Thereafter, cells were treatment with 10 mM LiCl, 10 mM NaCl and 100 ng/ml ultrapure LPS for 24 hrs, 10 µg/ml PMA and 10 µg/ml FMLP for 30 min. In addition, other cells were treated with a combination of the salts with the stimulant. Measurement of GSH was accomplished by GSH-Glo glutathione assay according to manufacturer's protocol. Thereafter, the produced luminescence was measured with GloMax-Multi microplate system (Promega, USA).

3.10 Effects of lithium on the expression of NF-κB signalling related genes in PMA stimulated Raw 264.7 macrophages.

Measurement of effects of lithium on the expression of NF-κB signalling pathway related genes was accomplished with Real Time PCR, the Raw 264.7 cells were stimulated with PMA in this regard. The C_t values from the Real Time PCR array were used to establish the dot plot (fig 3.16), that is used to estimate the variation in gene expression comparing untreated control with 10 mM LiCl and PMA. Treatment with lithium chloride led to an upregulation of NF-κB1/p50, NF-κB2/p52, Jun, c-Rel, RelB, RelA/p65 and Bcl3 in PMA stimulated cells (fig 3.17 A). The expression of NF-κB1/p50, Bcl3, Jun and c-Rel was elevated in combinatory treatment as compared to PMA treatment. Moreover, expression of RelB and RelA/p65 is less in the combinatory treatment as compared to PMA treatment (fig 3.17 A). An increase in the expression of IκB-ε, Chuk and NFκBia/IκB-α was observed in PMA treated cells as well as in cells treated with a combination of lithium chloride and PMA but to a less extent as compared to PMA. Figures 3.17 C, shows expression of Mapk3, Tollip and Traf3 in all treatments, but more expression of these proteins are observed in 10 mM LiCl and combinatory treatment as opposed to PMA, in addition combinatory treatment shows expression of Akt1. Furthermore, figure 3.17 D recognises upregulation of TNF and IL1b in PMA and combinatory treatment.

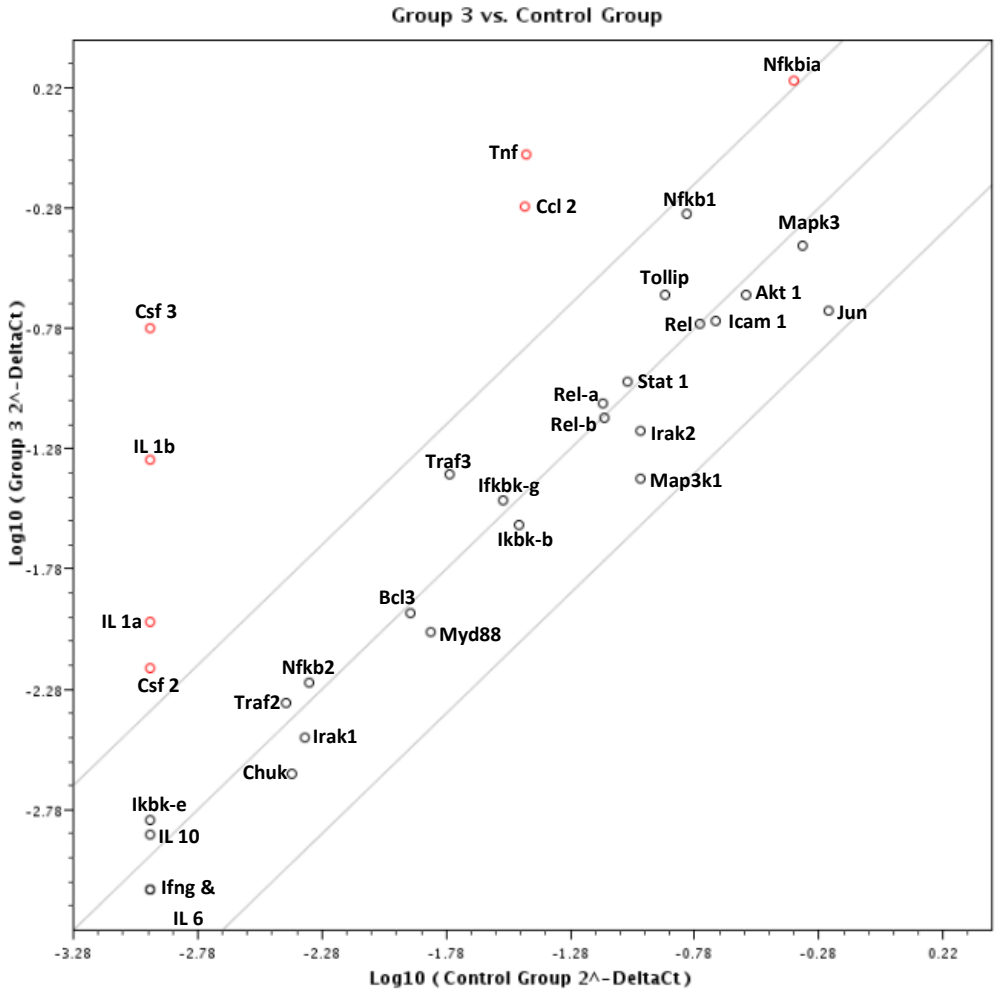

Figure 3.16: Expression of the NF-κB signalling related genes as shown by the Dot plot. Raw 264.7 cells were cultures at a density of $6x10^6$ cell/ml in a 60 mm cell culture dishes. Thereafter, cells were treated with 10 mM LiCl, 10 µg/ml PMA and a combination of the lithium with the PMA stimulant for 24 hrs, but the stimulant went for 30 min. Total RNA isolation was accomplished with qiagen Total RNA isolation kit, cDNA was synthesised with RT^2 Fist strand kit. RT^2 profiling PCR Arrays were used to measure the expression profiles and the C_t values from qiagen data analysis website were used to develop the dot plot.

A

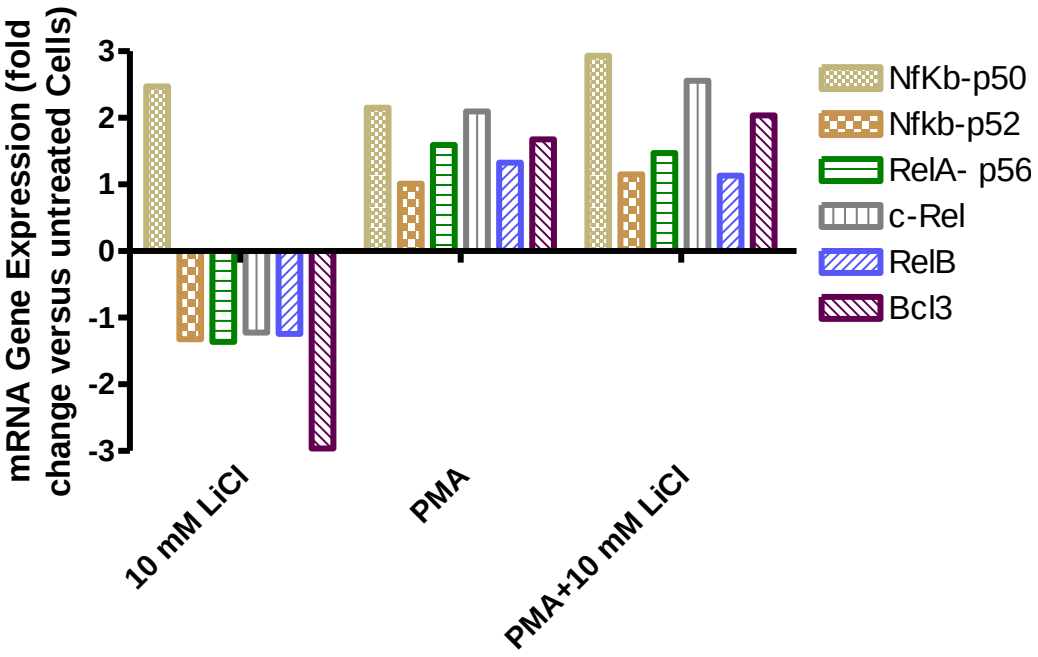
mRNA Gene Expression (fold change versus untreated Cells)
3
2
1
0
-1
-2
-3
10 mM LiCl
PMA
PMA+10 mM LiCl
NfKb-p50
Nfkb-p52
RelA- p56
c-Rel
RelB
Bcl3

B

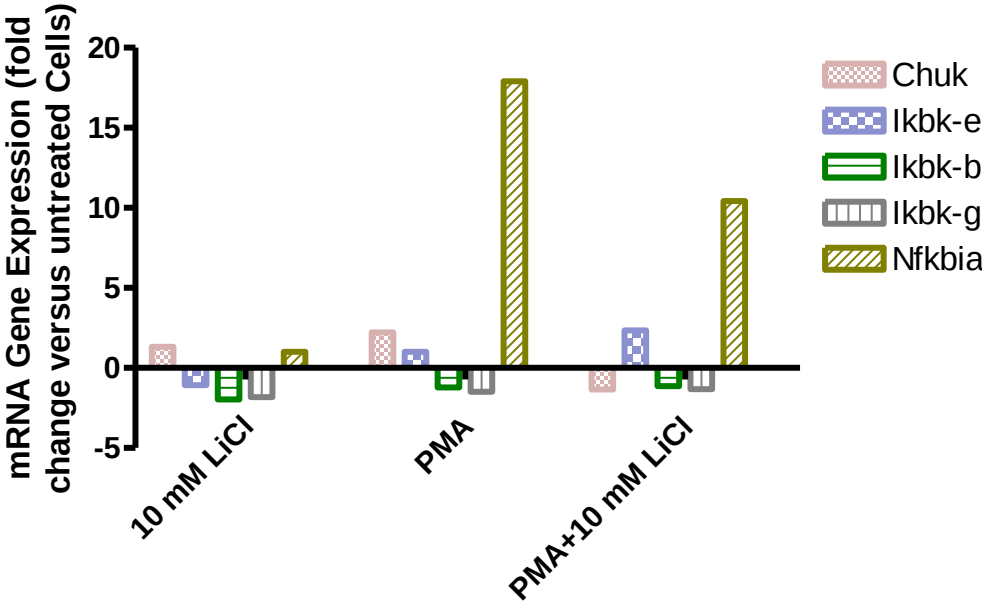
mRNA Gene Expression (fold change versus untreated Cells)
20
15
10
5
0
-5
10 mM LiCl
PMA
PMA+10 mM LiCl
Chuk
Ikbk-e
Ikbk-b
Ikbk-g
Nfkbia

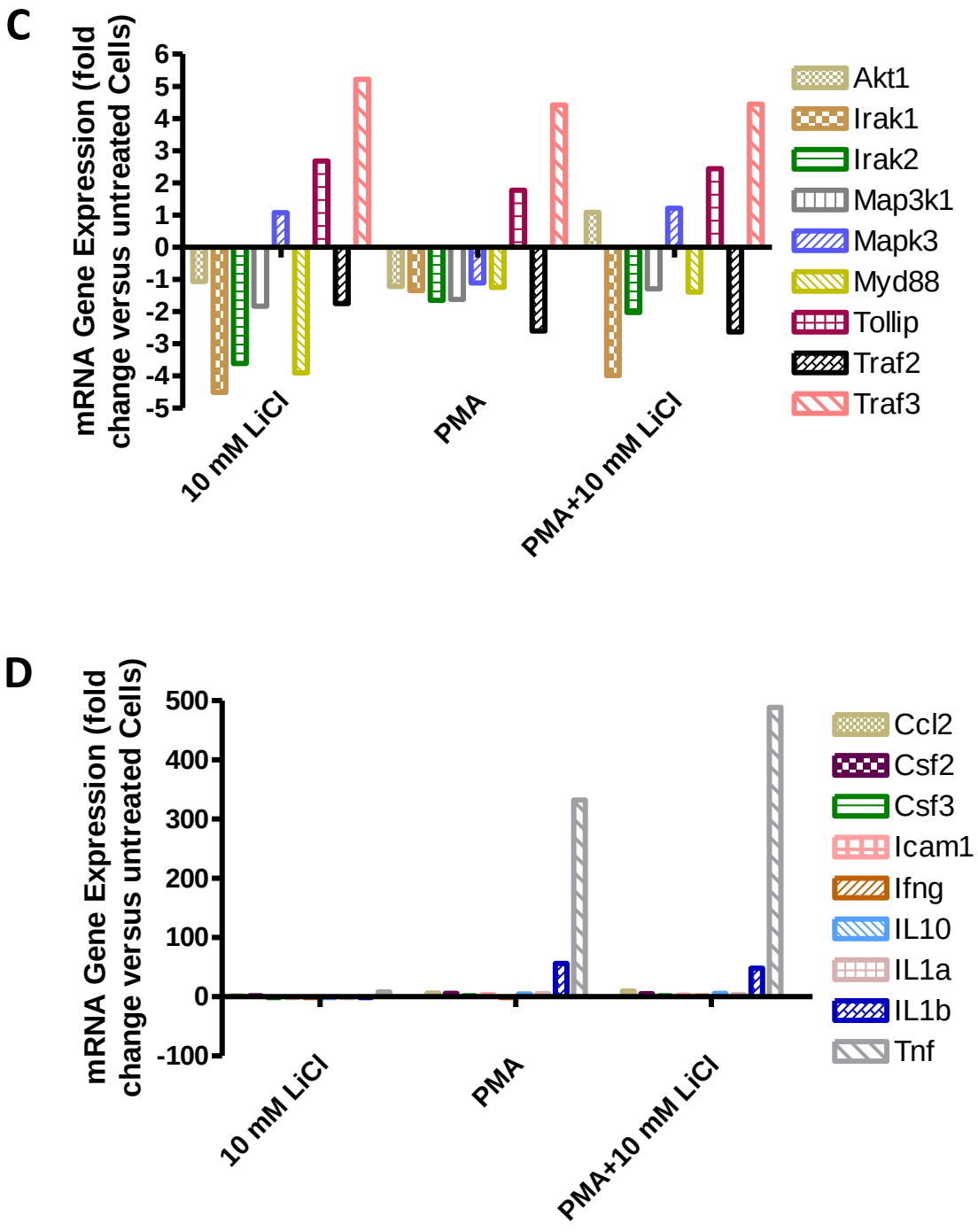

Figure 3.17: Effects of lithium on the expression profiles of NF-κB signalling related genes in Raw 264.7 macrophage cells activated with PMA. Raw 264.7 cells were cultured in a 60 mm cell culture dishes at a density of $6X10^6$ cell/ml. Thereafter, cells were treated with 10 mM LiCl, 10 µg/ml PMA as well as combination of the lithium salt with the stimulant for 24 hrs, but the stimulant went for 30 min. RT^2 profiling PCR Arrays were used to measure the expression profiles of NF-κB were in which 40 cycles where accomplished and then qiagen web based data analysis, was used to analyse the C_t values and then graph pad prism was used to plot the graphs.

3.11 Lithium inhibits oxidative burst as stimulated by FMLP on Raw 264.7 macrophages

The anti-inflammatory role played by lithium was further evaluated on Raw 264.7 macrophages using FMLP as a stimulant. Treatment with lithium chloride was seen to lower the fluorescent intensity in FMLP-stimulated cells in comparison with FMLP treated cells. This was further confirmed by the use of NIS Element view imaging software (NIKON, Japan), which showed significant amongst the FMLP treatment and combinatory treatment (FMLP and 10 mM LiCl) (fig 3.18).

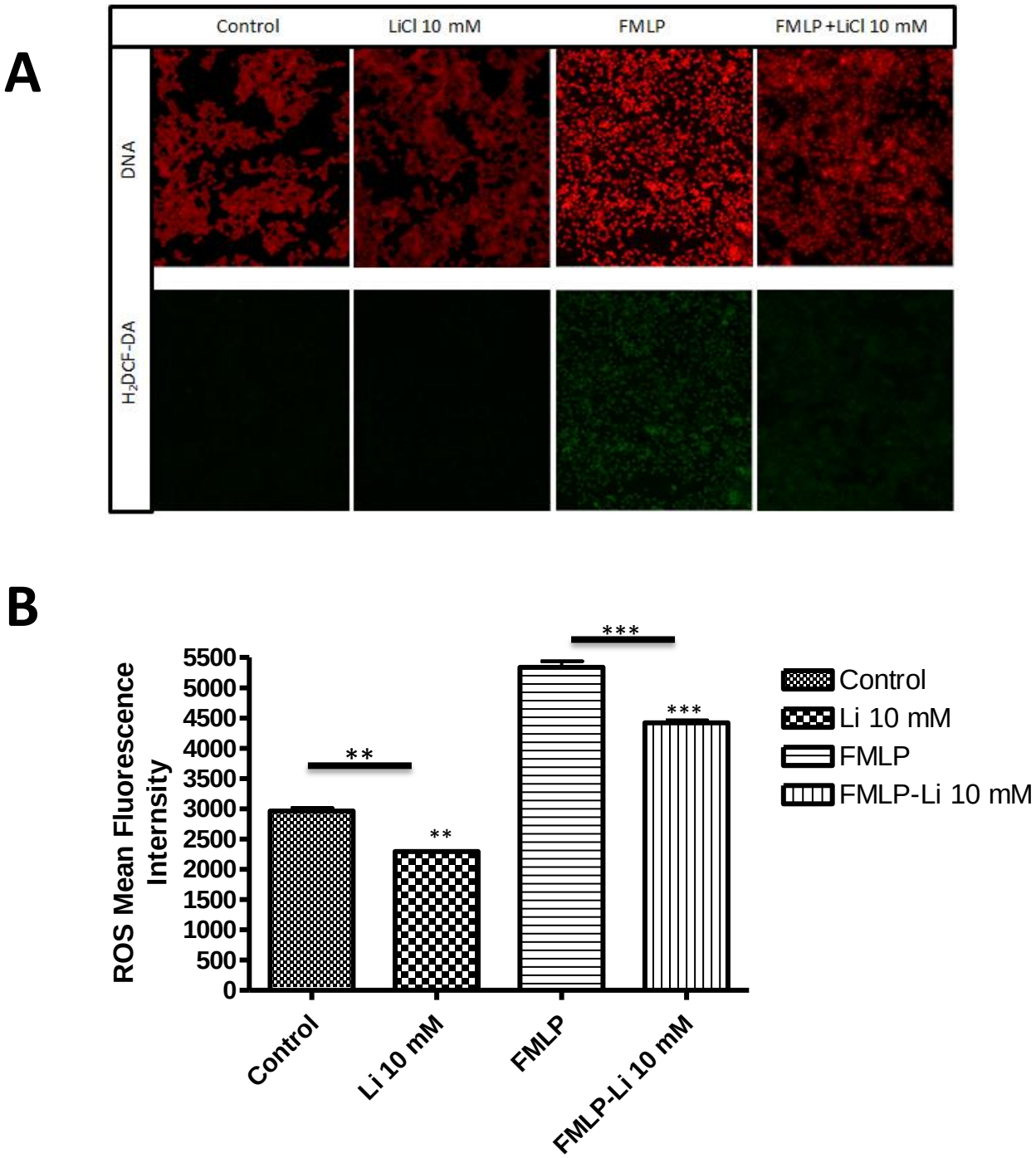

FIGURE 3.18: Effect of lithium on oxidative burst stimulated by FMLP on Raw 264.7 macrophage cells. Raw 264.7 macrophage cells were seeded at a density of $6x10^5$ cells/ml on a coverslip and then pre-treated with 10mM LiCl for 24hrs and stimulated with 10 nM/ml FMLP for 30 min. The slides were analysed Ti-E inverted microscope at [A], and then fluorescence intensity of the pictures was measured using the NIS Element view imaging software (NIKON, JAPAN). The numeric data was then used to plot the graph with Graph pad prism-4 software [B].

3.12 Effects of lithium on production of Glutathione by Raw 264.7 macrophages following FMLP stimulation

The production of GSH after FMLP stimulation was measured using the GSH measurement assay. The presence of this molecule was determined through conversion of a luciferin derivative into luminescent luciferin in the presence of glutathione, catalyzed by glutathione S-transferase (GST). The results showed an increase in the production of GSH in cells treated with lithium including the combination treatment 10 mM lithium chloride and FMLP (fig 3.19).

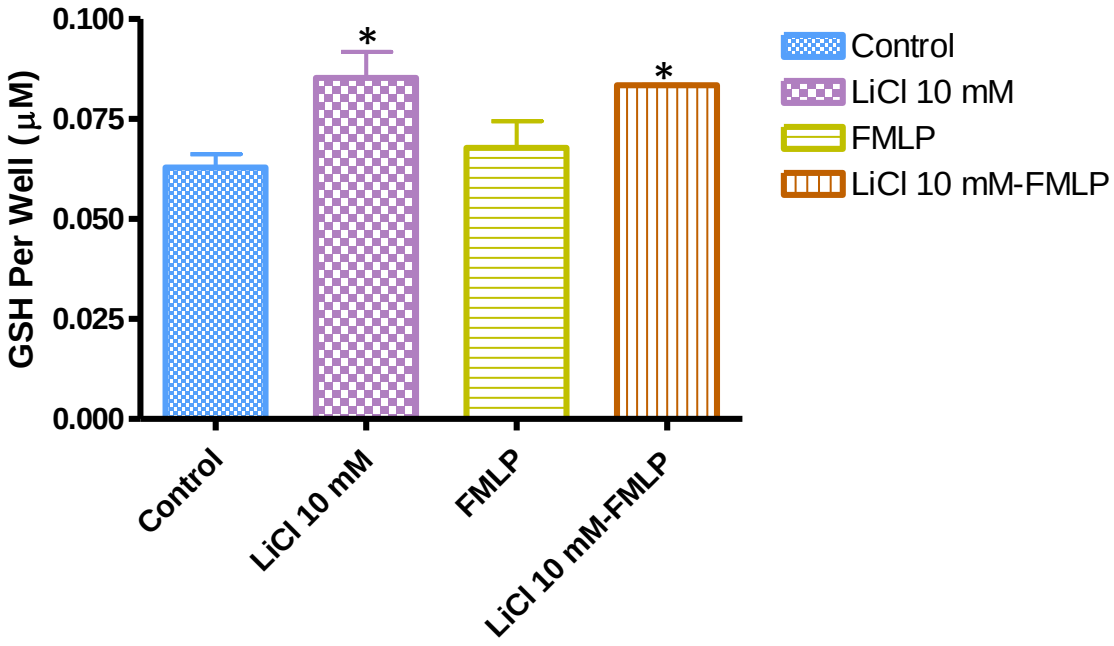

Figure 3.19: Effects of lithium on the production of Glutathione in FMLP stimulated Raw 264.7 macrophages Raw 264.7 cell, cell were culture at a density of 10 000 cells/ml and then treated the cells with 10 mM LiCl and 10µg/ml FMLP for 30 min. In addition, other cells were treated with a combination of the salts with the FMLP stimulants. Measurement of GSH was accomplished by GSH-Glo glutathione assay according to manufacturer's protocol. Thereafter, the produced luminescence was measured with GloMax-Multi microplate system (Promega, USA).

3.13 Effects of lithium on expression of NF-κB signalling related genes after FMLP stimulated Raw 264.7 macrophages

The Real Time PCR array was used to evaluate the expression profiles of NF-κB related genes after FMLP stimulation of Raw 264.7 macrophages. The dot plot shows a general map of expression profiles of analysed genes generated using qiagen web based data analysis comparing 10 mM lithium chloride and 10 mM lithium chloride with FMLP (fig 3.20). Figure 3.20 B showed the expression of IκB-ε in FMLP treatment and then figure 3.20 A show up-regulation of NF-KB1/p50 in 10 mM LiCl. The Traf3 and Tollip proteins are up-regulated in cells treated with 10 mM lithium chloride and combination treatment (10 mM LiCl and FMLP). Moreover, figure 3.20 D show some positive expression of this molecules Csf2, IL1-A, IL6, IL1-B, TNF-α, CSF3 (granulocyte colony stimulating factor 3) and Ccl2. All of these proteins are observed in FMLP treatment except Ccl2, while lithium treatment show positive expression of Ccl2, Csf3. These results (fig 3.20 D) showed overexpression of Tumor necrosis factor (TNF) in lithium chloride treatment as well as the combination treatment.

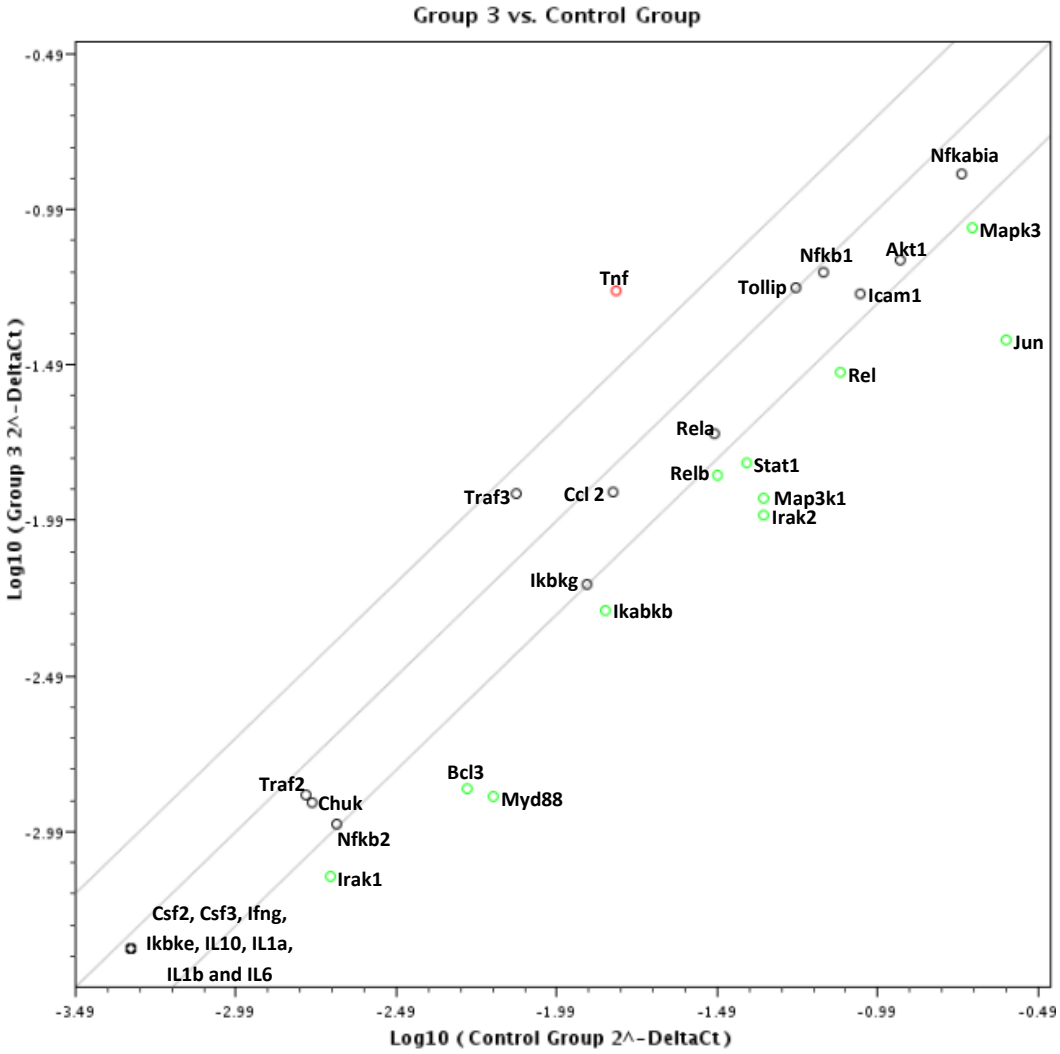

Figure 3.20: The expression profiles of NF-κB signalling related genes as illustrated by the Dot plot. Cells were cultures at a density of of 6X10^6 cell/ml in a 60 mm cell culture dishes and then treated with 10 mM LiCl, 10 µg/ml FLPM and a combination of the lithium with the FMLP stimulant for 24 hrs, but the stimulant went for 30 min. Total RNA isolation was accomplished with qiagen Total RNA isolation kit, cDNA was synthesised with RT^2 Fist strand kit. RT^2 profiling PCR Arrays were used to measure the expression profiles and the C_t values were used to determine the expression profiles of NF-κB signalling related genes. The dot plot was developed with the C_t values using the qiagen data analysis website.

A

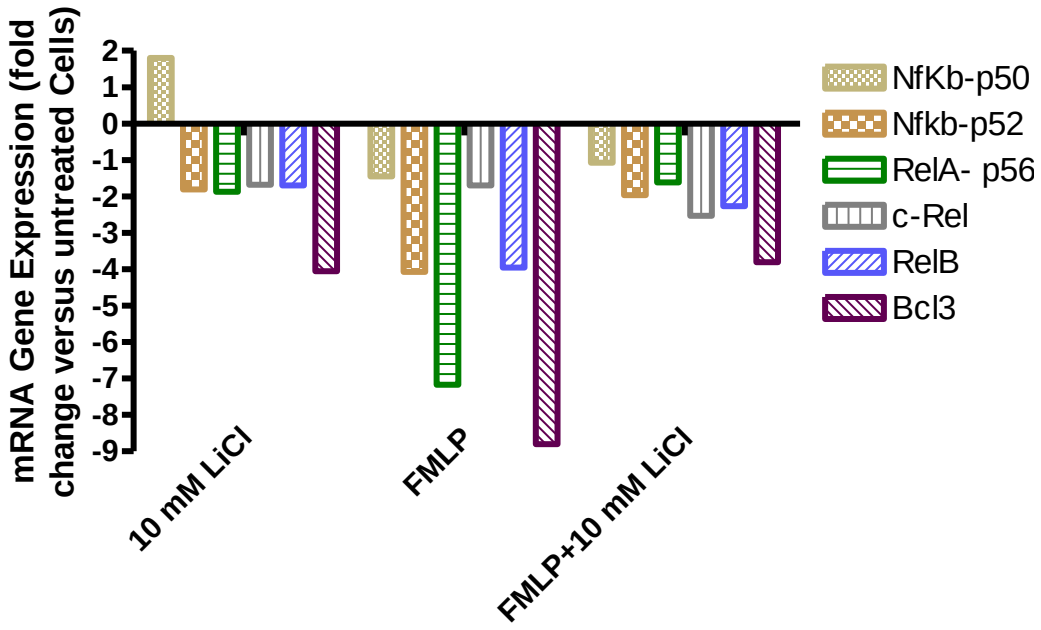
mRNA Gene Expression (fold change versus untreated Cells)
2
1
0
-1
-2
-3
-4
-5
-6
-7
-8
-9
10 mM LiCl
FMLP
FMLP+10 mM LiCl
NfKb-p50
Nfkb-p52
RelA- p56
c-Rel
RelB
Bcl3

B

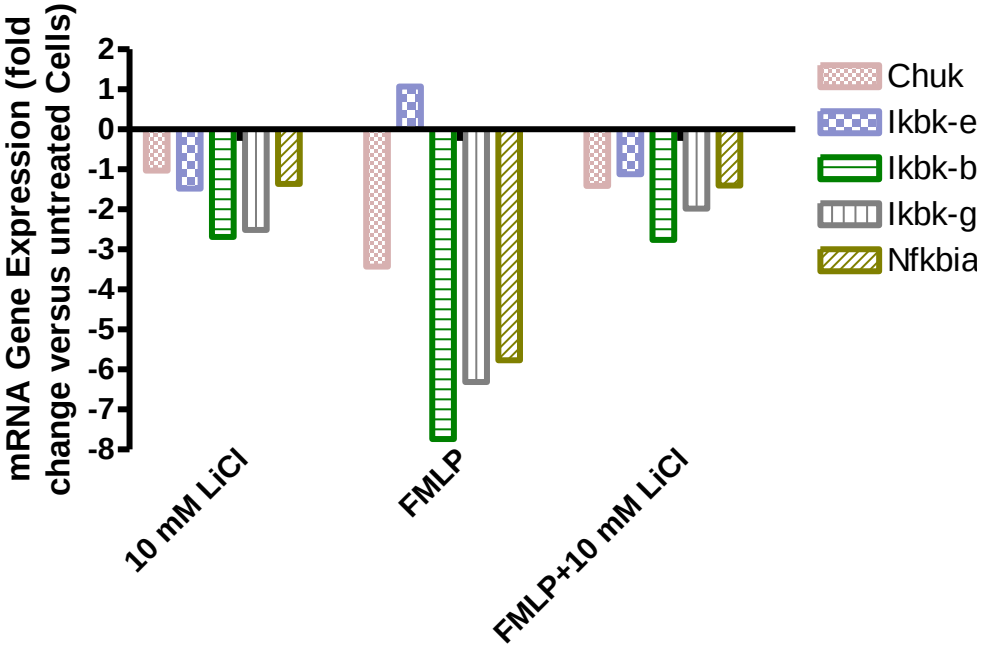
mRNA Gene Expression (fold change versus untreated Cells)
2
1
0
-1
-2
-3
-4
-5
-6
-7
-8
10 mM LiCl
FMLP
FMLP+10 mM LiCl
Chuk
Ikbk-e
Ikbk-b
Ikbk-g
Nfkbia

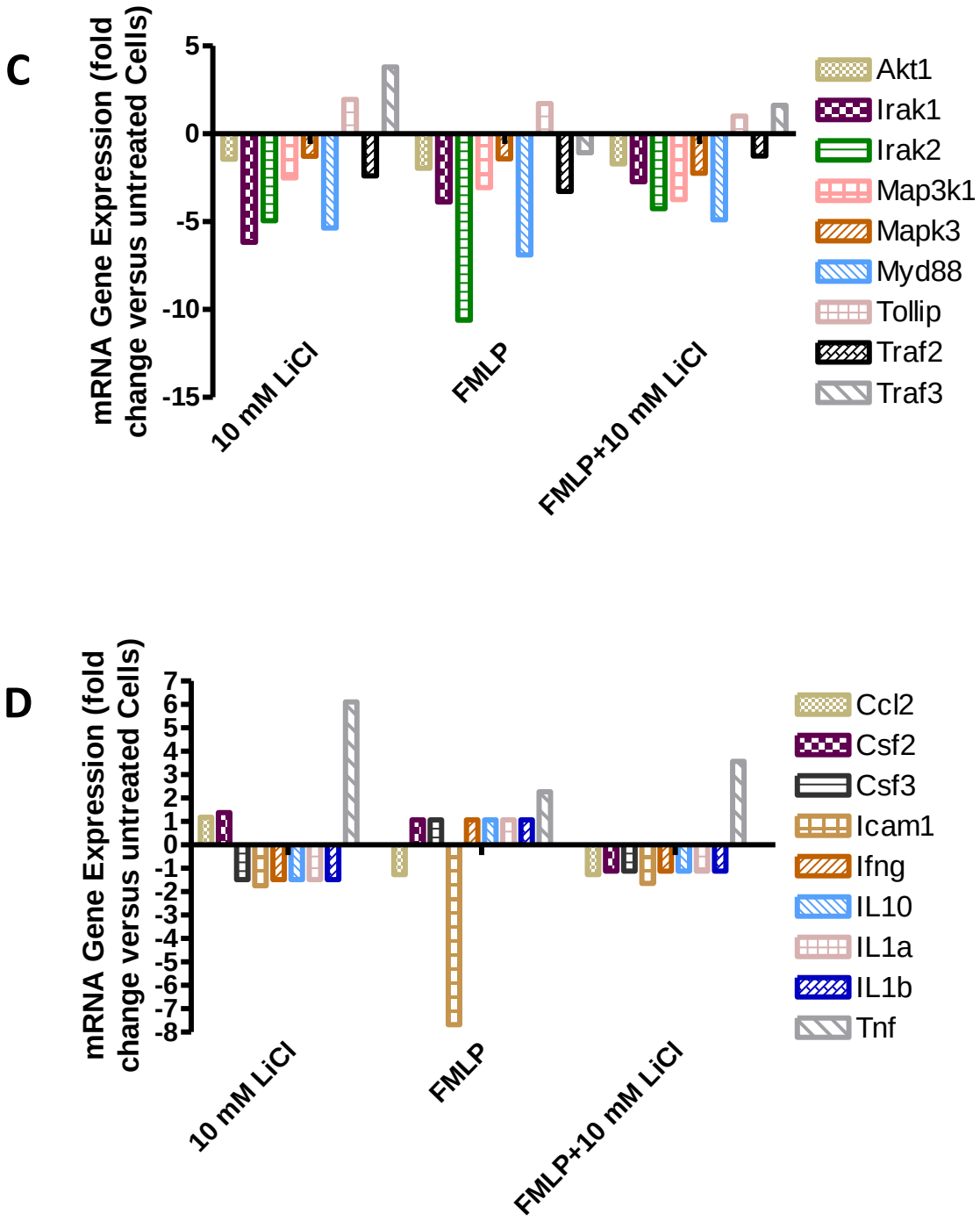

Figure 3.21: Effects of lithium on expression profiles of NF-κB signalling related genes on Raw 264.7 macrophage cells activated with FMLP. Raw 264.7 cells were cultured in a 60 mm cell culture dishes at a density of $6X10^6$ cell/ ml and then treated with 10 mM LiCl, 10 µg/ml FMLP as well as combination of the lithium salt with FMLP for 24hrs and/ or for 30 min. Total RNA isolation was accomplished with qiagen Total RNA isolation kit, with cDNA synthesised with cDNA synthesis with

RT^2 Fist strand kit. RT^2 profiling PCR Arrays were used to measure the expression profiles of NF-κB were in which 40 cycles where accomplished. Thereafter, qiagen web based data analysis, was used to analyse the C_t values and then graph pad prism was used to plot the graphs.

CHAPTER FOUR

DISCUSSION

Inflammation is a defence mechanism used to combat deleterious agents such as bacteria, fungi, viruses and toxins that invade the mammalian immune system. This process is accomplished by the use of pattern recognition receptors such as Toll like receptors (TLR) on the innate immune cells, which recognise pathogen associated molecular patterns on the antigen. The activated receptors recruit adaptor molecules (e.g. Myd88) leading to the activation of some kinases downstream and eventually transcription factors such as NF-κB and AP-1 which results in the elicitation of an immune response. Despite the beneficial outcomes of inflammation, this process requires constant and tight regulation since its deregulation could be harmful to the host (Didierlaurent *et al*., 2006).

A body of experimental evidence has outlined the detrimental consequences as a result of dysregulated activation of the inflammatory transcription factors mentioned above. The consequences involve vast production of ROS that impairs proteins, lipids and nucleic acids which eventually leads to the generation of diseases and disorders (Jope *et al*., 2006). Currently used anti-inflammatory agents present challenges such as severe neuronal-associated side effects manifesting in patients. On the other hand, lithium is well-known to protect neuronal cells against cytotoxicity and has been used for more than 6 decades in the treatment of bipolar disorders (Khasraw *et al.,* 2012). Thus, this study investigated the use of a naturally occurring trace element, lithium, in the treatment of prolonged and acute inflammatory response. Lithium is an alkali metal and a monovalent trace element naturally found in various concentrations in grains, vegetables and drinking water (Suganthi *et al*., 2012; Strunecká *et al*., 2005).

This metal was discovered as a salt in 1817 by Johan August Arfwedson (Strunecká *et al*., 2005). Moreover, in 1949, Cade discovered the medical significances of lithium in humans suffering from psychiatric disorders (Cade, 1949). Thus, this drug was used as a preferred, gold standard treatment for bipolar disorders, despite its mysterious mode of action (Cade, 1949; McKellar, 2007). The use of this drug has led to reduced need for hospitalization and prevention of manic episodes in individuals with bipolar disorder, depression, schizophrenia and cyclothymia (Birch *et*

al., 1993). Majority of scientific work done with lithium has been accomplished in neuronal cells as opposed to any other cell types, in an attempt to comprehend the mechanism in which lithium calms manic episodes (Allagui *et al*., 2008; Khasraw *et al.,* 2012; Yeste-velasco *et al*., 2008).

Although lithium chloride, at 10 mM, was reported to have selective cytotoxicity towards HL-60 cancer cells while sparing non-cancerous cells (Becker and Tyobeka, 1990; Mampuru *et al.,* 1999, and Matsebatlela *et al.,* 2000), the cytotoxic effects of lithium chloride on Raw 264.7 macrophage cells is unknown. Macrophages are known to be the first line of defence, since they play a central role in coordination of innate immunity and inflammation (Taylor *et al*., 2005). Thus, this study explored the cytotoxic spectrum of lithium chloride on Raw 264.7 mammalian macrophages and NIH 3T3 fibroblast cells lines by monitoring cell growth and proliferation after LiCl treatment. The results showed that lithium Chloride, up to 20 mM, is non-cytotoxic to Raw 264.7 cells as determined by MTT viability assay and xCELLigence real time analyser system (fig 3.1 and 3.3). Similar results were observed when NIH 3T3 fibroblast cells were exposed to 10 mM LiCl (fig 3.2).

In addition to the cell cytotoxicity assays, cell imaging and Annexin V and PI staining revealed no signs of apoptosis induced by 10 mM lithium chloride in Raw 264.7 and NIH 3T3 cell lines. (fig 3.4, and 3.5). A flow cytometry assay was used as a quantitative method to evaluate the apoptotic signs of lithium chloride. This system analyse every single cells within a certain gated cell population. This assay as well showed the non-apoptotic properties of 10 mM lithium chloride on Raw 264.7 cell line, where in which 5- 20 mM LiCl treated cells showed negative staining with Annexin-V and PI. Lithium chloride treatments of 5 to 20 mM are said to be non-apoptotic since majority of their cell count resides in the negative quadrant bottom left as denoted by quadrant statistics 92.53%, 85.49%, 83.65% respectively (fig 3.6 B, C & D).

Conversely, treatment of cells with actinomycin-D (0.01 and 0.02 mg/ml) led to the induction of apoptosis as evidenced by the positive staining of cells with both Annexin-V and PI and they are localised in the top right quadrant (quadrant stat 38.25% and 39.35%) respectively. Therefore, this data suggests that lithium chloride at concentrations up to 20 mM does not impede cell growth, proliferation nor change

the spindled shaped morphology of Raw 264.7 and NIH 3T3 cell lines. In addition to the non-cytotoxicity, lithium chloride at 20 mM and below doses was shown to be unable to induce programmed cell death. This data supports the claim that lithium chloride may be selectively cytotoxic in killing the cancerous cell while sparing the normal cells (Becker and Tyobeka, 1990; Mampuru *et al.,* 1999, and Matsebatlela *et al.,* 2000). Moreover, this data supports the reliable safe use of lithium in clinical health and its hematopoietic role (Barr and Galbraith, 1983).

Studies (Khasraw *et al.,* 2012 and Freland and Beaulieu, 2012) have shown that lithium has both neuroprotectivity and pro-survival properties in various cell types. Lithium is thought to accomplish this role due to its ability to inhibit glycogen synthase kinase-3 (GSK-3) which positively regulates the stability of β-catenin. Therefore, the stable β-catenin binds to Tcf-Lef family of transcription factors. Tcf-Lef transcription factors induce expression of survival/ proliferation promoting genes such as cyclin-D1 and insulin-like growth factor-II (IGF-II) (Freland and Beaulieu, 2012). In addition to the putative survival and protective properties of lithium via GSK-3 and Akt (Freland and Beaulieu, 2012; Kang *et al*., 2003), lithium is known to inhibit NF-κB, the vital inflammatory molecule (Zhang *et al*., 2008).

Rel/NF-κB is a pleiotropic transcription factor known to be involved in several signalling pathways namely; inflammation, proliferation, growth, differentiation, apoptosis and angiogenesis (Barnes and Karin, 1997; Moynagh, 2005). Rel transcription factor describes a family of proteins that form dimers, which have a conserved N-terminal, the rel homology domain (RHD) (May and Ghosh, 1997). This family consist of five proteins subunits namely: NF-κb1/p50, NF-κB2/p52, c-Rel, RelA/p65 and RelB that form hetero and/or homo-dimers, which results in an active transcription factor (Moynagh, 2005). The NF-κB transcription factor is predominant within the cytosol in resting cells and complexes with inhibitor of kappa B (IκB) proteins (Barnes and Karin, 1997).

This study emanates from the proposed link between oxidative stress and chronic ailments such as neurodegeneration, diabetes, cancer and inflammatory bowel like diseases (Barnes and Karin, 1997; Jope *et al*., 2007). Results of this study showed that lithium at low doses significantly lowers NO production stimulated by LPS using Griess and DAF2-DA NO detection assays (fig 3.7 and 3.8). Nitric oxide production

is significantly lowered in cells that are treated with low concentrations of lithium chloride and LPS as compared to LPS only. In addition to NO production inhibition shown by low doses of lithium chloride, phagoburst assays revealed that 10 mM LiCl down-regulates ROS production after LPS stimulation (fig 3.9 A & B). Lipopolysaccharide (LPS) was used as an inflammatory stimulant since it is known to activate macrophages by modulating the activity of NF-κB via toll-like receptor-4 (Gordon, 2007).

The anti-inflammatory properties shown by 10 mM LiCl in LPS stimulation prompted the use of other stimulants such as PMA and FMLP in an attempt to investigate other inflammatory related pathways. Phorbol 12-myristate 13-acetate (PMA) mimics diacylglycerol and it induces oxidative burst by activating MAP-kinases and Ap-1, whereas FMLP function as a chemokine inducing macrophages phagocytic activity. The use of these stimulants has further revealed that 10 mM LiCl significantly ($p<0.05$) lowers ROS production (fig 3.14 and 3.18). Thus, the proposed anti-inflammatory properties illustrated by lithium lead to investigation of its biochemical mode of action which involved examination of NF-κB signalling pathway and non-enzymatic antioxidant Glutathione (GSH) levels. The investigation of GSH level production showed that 10 mM LiCl significantly up-regulates production of GSH (fig 3.10, 3.15, 3.19). This assay revealed significant distinction in GSH production between 10 mM LiCl, untreated control and stimulants (LPS, FMLP and PMA).

The non-enzymetic anti-oxidant GSH is known to be a co-factor of some enzymes such as GSH S-transferase (GST) and GSH peroxidase (GPx) (Cui *et al*., 2007). This molecule is known to exist in high amounts in the neuronal cells since brain metabolism requires high amounts of oxygen resulting in production of free radicals. Thus, alteration in the production of these molecules prone brain to oxidative damage leading to brain disorders such as Parkinson's diseases (Cui *et al*., 2007; Townsend *et al.,* 2003). More studies have shown that the suggested neuroprotective property of lithium pertains to stimulation of GSH. These studies have evaluated the neuroprotective properties of lithium on primary cultured rat cerebral cortical cells and they have shown that GSH inhibitor (buthionine sulfoximine) alter the neuroprotective property elucidated by lithium as opposed to lithium treated cerebral cells (Cui *et al*., 2007; Townsend *et al.,* 2003).

These findings suggest that lithium might be stimulating the Nrf-2 transcription factor most probably via GSK-3β. Nuclear factor erythroid 2-related factor (Nrf-2) resides in the cytoplasm coupled with keap proteins in resting cells and translocate to the nucleus in response to oxidative and electrophilic stress. This transcription factor is regulated upstream by GSK-3β which is known to be a target of lithium (Jain and Jaiswal, 2007). Therefore, to find the insight of lithium mode of action on the anti-oxidant response signalling, more work is required to reinforce this suggestion. In addition, to the GSH production role of lithium chloride, immunocytochemistry assay suggest that 10 mM lithium chloride minimises or revers the translocation of Rel-A /p65 in the nucleus after LPS stimulation. This inference is based on the green fluorescence signal observed in both the nucleus and cytosol as compared to untreated control and 100 ng/ml LPS (fig 18).

The Real Time PCR profiler arrays links the anti-inflammatory property of lithium chloride with upregulation of IκB-α, TRAF3, Tollip and NF-κB1/p50. These genes are up-regulated by the addition of lithium chloride as shown by the Real Time PCR bar plots and the dot plot that shows a map of overexpressed and under-expressed genes comparing control and combination of LiCl and stimulant (LPS, PMA and FMLP) (fig 3.12, 3.16 and 3.20). The IκB-α is known to block the DNA-binding of NF-κB dimers (p65-p50) using its DNA dissociation abilities that lies on the C-terminal of the IκB-α (May and Ghosh, 1997). In normal stimulated cells, this inhibitor revers the inflamed condition in order to regulate inflammation since, unregulated persistent inflammation becomes harmful to the host (Didierlaurent *et al*., 2006). Therefore, the Raw 264.7 cell express this inhibitor but the expression appears to be more in combinatory treatment that encompasses 10 µg/ml LPS/ PMA and 10 mM LiCl (fig 3.13 B and 3.17 B) in addition to IκB-α this treatment expresses the IκB-ε.

Furthermore, this study observed up-regulation of NF-κB1/p50 mostly in 10 mM LiCl and stimulant (LPS and PMA) with 10 mM LiCl treatments (fig 3.17 A and 3.13 A). In addition to the inhibitory role of IκB-α this study suggests that p50 homodimer may inhibit the transcriptional role of p50-p56 heterodimer. This inference is supported by the experimental evidence (Udalova *et al*., 2000; Perkins *et al*., 1992) that has shown that p50 homodimer act as transcriptional repressor since it is known to possess the DNA binding domain but not the transcriptional activation domain. The p50 homo dimer is thought to compete for kappa responsive site with p65-p50 dimer.

Other findings linked the interaction of the p50 homodimer with dorsal switch protein 1 which gives p50 homodimer its repressive property (Udalova *et al*., 2000).

Tollip is the other inhibitory gene that is up-regulated by lithium treatment, this gene is up-regulated in 10 mM LiCl and stimulant (LPS, FMLP and PMA) with 10 mM LiCl treatments (fig 20C, 24C & 28C). Tollip proteins are known to arrest immune cells in quiescent state in the absence of infection or stimulant. Tollip proteins are said to impair IL-1R, TLR-2 and TLR-4 and the activation of innate immunity and ROS production. Tollip protein dissociates from interleukin-1R associated kinase 1 (IRAK1) thereby bridging the signal downstream, thus failure to dissociate from IRAK1 facilitates inactivation of NF-κB and JNK leading to ROS inhibition downstream (Didierlaurent *et al*., 2006). In addition to expressed Tollip, this study observed the up-regulation of TNFR-associated factors 3 (TRAF-3), more in 10 LiCl and stimulant (LPS, FMLP and PMA) with 10 mM LiCl.

A TNFR-associated factor 3 (TRAF-3) has shown some inhibitory role as studied in Lymphotoxin Beta Receptors (LTBR) or Tumor necrosis factor related receptors, this molecule inhibits the NF-κB/p52 through inhibition of NF-κB-inducing kinase (NIK) that is required to process p100 to active p52 (Bista *et al.,* 2010). Furthermore, Bista *et al* 2010 show that TRAF-3 inhibits the NF-κB/p50 and the recruitment of TRAF-2 and IKK to the LTBR induced signalling complex. Study by Bista *et al* 2010 show LTBR signal-dependent activation of NF-κB2 that degrades TRAF3 and leading to stabilization of NIK (Bista *et al.,* 2010).

Recent findings showed that inflammation plays a central role in bipolar disorders, thus most of studies have focused on the effects of cytokines in these disorders (Guloksuz *et al*., 2012). Clinical and pre-clinical studies showed that lithium down regulate the pro-inflammatory cytokines such as TNF-α, IL-1β, IL-6 and PGE_2, while up-regulating the anti-inflammatory cytokines such as IL-10 and IL-4. In addition, these studies have observed upraised activity of superoxide dismutase and levels of GSH (Albayrak *et al*., 2013; Guloksuz *et al*., 2012). The current work also has observed the down-regulation of pro-inflammatory cytokine gene expression such as Ifn-g, IL-10, IL1-α and IL1-β after lithium treatment (fig 3.13D, 3.17D, 3.21D).

The results of this study suggested the anti-inflammatory properties of lithium as studied using phagoburst, Griess, GSH-Glo assay and DAF2-DA assays, thus these

results lead to the investigation of lithium's mechanism of action. The immunocytochemistry then showed the reversal of the vital inflammatory transcription factor NF-κB (p50-p65 dimer) by lithium. Real Time PCR results suggest the putative mode of action of lithium to involve the up-regulation of regulatory inflammatory genes outlined above, albeit the sequence of events it's unknown. This study suggests inhibition of p65-p50 dimer and down-regulation of ROS production to occur via up-regulation of p50, IκB-α, IκB-ε, TRAF-3 and Tollip genes.

The expression of these inhibitory molecules is thought to be the reason the cells treated with both LPS and LiCl in the immunocytochemistry revers translocated NF-κB as evidenced by a green signal in both the cytoplasm and nucleus. Up-regulation of p50 subunits by lithium compliments the proliferative characters that lithium possesses, since p50 homodimers were known to be involved in B-cell development (Moynagh, 2005). In addition to these genes, lithium as well up-regulates the Traf-3 that destabilizes NIK that is required to activate p50 and p52 by removing the C-terminal of p100 and p105 respectively (Bista *et al.,* 2010).

This work suggests that lithium chloride show inhibitory/ anti-inflammatory role through expression of the antioxidant (glutathione) and through expression of the above mentioned inhibitory genes. Inflammation is thought to be at the centre of most of the chronic diseases, thus, inflammatory solution will result in solution of most of the chronic ailments. Using lithium as a drug of choice will be accessible to a wide population of our communities and the world at large. The study has realised that protein expression studies are required to strengthen the mRNA expression study that we currently have. Moreover, the inhibition study is required to elucidate the exact mechanism of action of lithium.

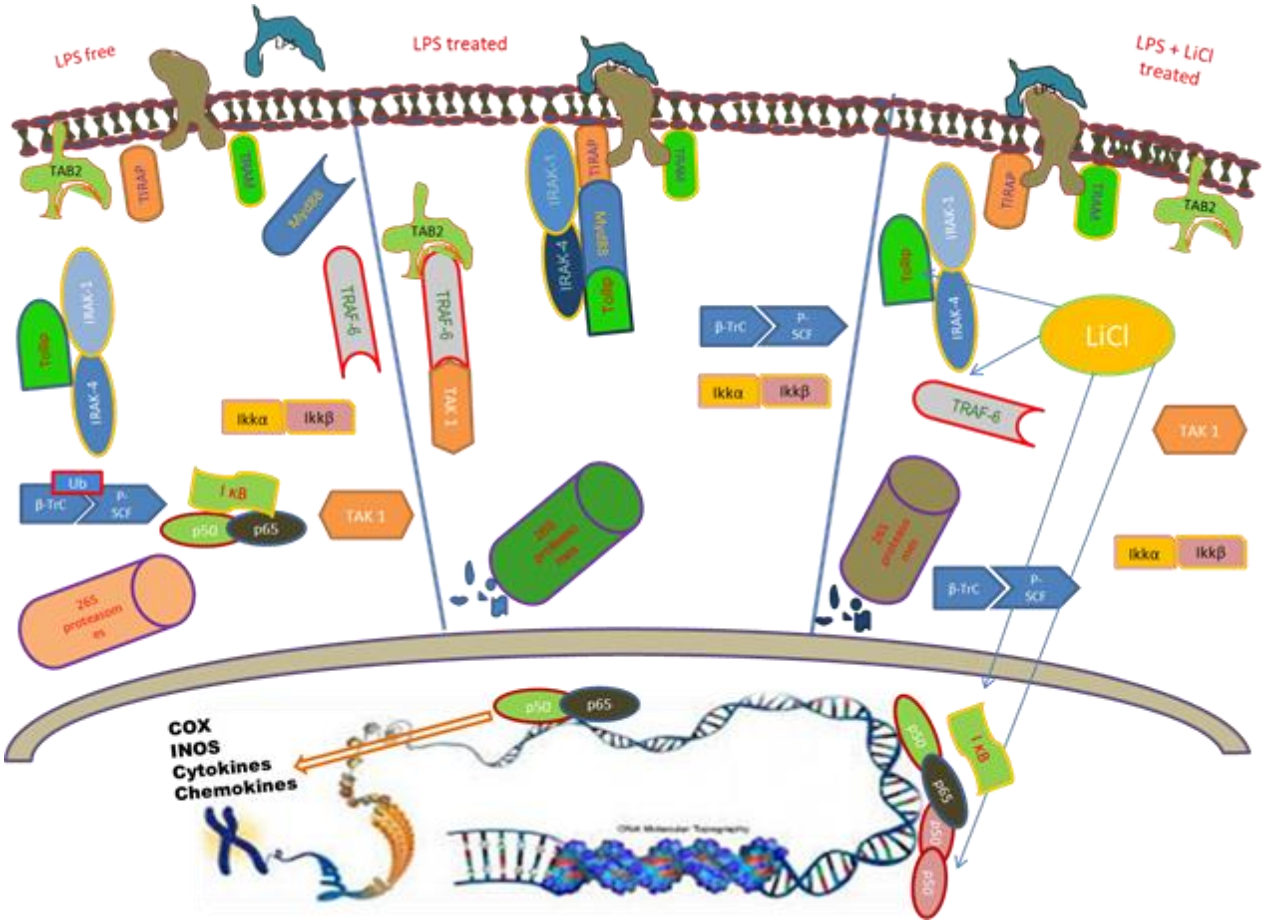

Figure 4.1: Demonstration of the putative mechanism of action of lithium in the NF-κB signalling pathway. The LPS free signalling involves the inhibition of the IRAK proteins in the cytoplasm by Tollip protein, this molecule is known to arrest immune cells in quiescent state in the absence of infection or stimulant. Thus, the inhibition of the IRAK proteins lead to the integrity of IκB then the entire signalling pathway is inhibited. In the LPS treatment the adapter molecule (Myd88) is recruited to the receptor, this then recruite the IRAK proteins in association with Tollip protein. Therefore the IRAK protein phosphorylates TRAF protein which recruits the TAB2 and TAK 1 which phosphorylates activate IKK. The IKK then phosphorylate the IκB, this molecule is then tagged for degradation by a ubiquitin. This sequence sequesters the NF-κB in the nucleus leading to expression of inflammatory genes. The combinatory treatment that include lithium chloride and LPS is thought to disturb the signalling pathway since lithium showed expression of some inhibitory proteins such as p50, IκB-α, NF-κB and Tollip (shown by arrows). These inhibitory molecules are the control points of the NF-κB signallaing pathway. The Tollip protein is thought to disturb the pathway by arresting the IRAK protein and then IκB-α removes the NF-κB from its responsive element by its DNA dissociation ability. Moreover, the p50 homo dimer competes for the responsive element with the NF-κB p50-p65 hetero dimer.

CHAPTER FIVE

REFERENCE

Albayrak A, Halici Z, Polat B, Karakus E, Cadirci E, Bayir Y, Kunak S, Karcioglu SS, Yigit S, Unal D, Atamanalp SS (2013) Protective effects of lithium: A new look at an old drug with potential antioxidative and anti-inflammatory effects in an animal model of sepsis. International Immunopharmacology. 16, 35–40.

Allagui MS, Nciri R, Rouhaud MF, Murat JC, Feki AE, Croute F, Vincent C (2008) Long-term exposure to low concentration of Lithium stimulates proliferation, modifies stress proteins expression pattern and enhances resistance to oxidative stress in SH-SY5Y Cells. J. Neuroche Res. 34, 453-462.

Barnes PJ, Karin M (1997) Nuclear Factor-kB — a pivotal transcription factor in chronic inflammatory diseases. The New England Journal of Medicine. 336: 1066-1071.

Barr RD, Galbraith PR (1983) Lithium and hematopoiesis. J. Can Med Assoc. 128, 123-126.

Becker RW, Tyobeka EM (1990) Lithium enhances proliferation of the HL-60 promyelocytic leukemia cells. Leukemia Res 14,879–884.

Bista P, Zeng W, Ryan S, Bailly V, Browning JL, Lukashev ME (2010) TRAF3 Controls Activation of the Canonical and Alternative NF-κB by the Lymphotoxin Beta Receptor. The journal of biological chemistry Vol. 285, 17, 12971–12978.

Birch NJ, Padgham C, and Hughes MS (1993) Lithium in medicine and biology. *Marius Press, Carnforth*, 616, 217-223.

Cade JFJ (1949) Lithium salts in the treatment of psychotic excitement. Medical Journal of Australia. 36, 349-352.

Candé C, Cecconi F, Dessen P, Kroemer G (2002) Apoptosis-inducing factor (AIF): key to the conserved caspase-independent pathways of cell death? *J. Cell Science*: 115, 4727-4734.

Cao Q, Lu X, Feng Y (2006) Glycogen synthase kinase-3β positively regulates the proliferation of human ovarian cancer cells. Cell Research 16, 671-677.

Chen CC, Chiu KT, Sun YT, Chen WC (1999) Role of the Cyclic AMP-Protein Kinase A Pathway in Lipopolysaccharide-induced Nitric Oxide Synthase Expression in RAW 264.7 Macrophages. The Journal of Biological Chemistry. 274, 31559–31564.

Christen Y (2000) Oxidative stress and Alzheimer disease. Am J Clin Nutr. 71, 621–629.

Cui J, Shao L, Young LT, Wang JF (2007) Role of glutathione in neuroprotective effects of mood stabilizing drugs lithium and valproate. Neuroscience 144, 1447–1453.

Didierlaurent A, Brissoni B, Velin D, Aebi N, Tardivel A, Kaslin E, Sirard CJ, Angelov G, Tschopp J, Burns K (2006) Tollip Regulates Proinflammatory Responses to Interleukin- and Lipopolysaccharide. Molecular and cellular biology Vol, 26. 3, 735–742.

Doble BW, Woodgett JR (2003) GSK-3: tricks of the trade for a multi-tasking kinase. Journal of Cell Science 116, 1175-1186.

Embi N, Rylatt D, Cohen P (1980) Glycogen synthase kinase-3 from rabbit skeletal muscle. Separation from cyclic-AMP-dependent protein kinase and phosphorylase kinase Eur. J. Biochem. 107, 519-526.

Ferlay J, Shin HR, Bray F, Forman D, Mathers CD, Parkin D (2010) GLOBOCAN 2008, Cancer Incidence and Mortality Worldwide. Int. J. Cancer. 127, 2893–2917.

Freland L, Beaulieu JM (2012) Inhibition of GSK3 by lithium, from single molecules to signalling networks. J. Frontiers in Molecular Neuroscience. doi: 10.3389/fnmol.2012.00014.

Fialkow L, Wang Y, Downey G.P. (2007) Reactive oxygen and nitrogen species as signaling molecules regulating neutrophil function. Free Radical Biology and Medicine; 42(2), 153-164.

Gookin JL, Chilang S, Allen J, Armstrong MU, Stauffer SH, Finnegan C, Murtaugh MP (2006) NF-κB-mediated expression of iNOS promotes epithelial defense against

infection by Crysporidium parvum in neonatal piclets. J Physiol Gastrointest Liver Physiol. 290, 164–174.

Guloksuz S, ltinbas K, Cetin EA, Kenis G, Gazioglu SB, Deniz G, Oral ET, J van Os (2012) Evidence for an association between tumor necrosis factor-alpha levels and lithium response. Journal of Affective Disorders. 143, 148‑152

Gordon S (2007) The macrophage: Past, present and future. Eur. J. Immunol. 37, S9–17.

Griess P (1879) Ber. Deutsch Chem. Ges. 12, 426.

Hancock JT, Desikan R, Neill SJ (2001) Role of reactive oxygen species in cell signalling pathways. Biochem. Soc. Trans. 29 (Pt 2), 345–350.

Jope RS, Yuskaitis CJ, Beurel E (2007) Glycogen Synthase Kinase-3 (GSK3): Inflammation, Diseases, and Therapeutics. J. Neurochem Res. 32, 577–595.

Jorge A. Quiroz, Todd D. Gould, Husseini K. Manji Mol Interv (2004) Molecular effects of lithium October; 4(5): 259–272. doi: 10.1124/mi.4.5.6

Kang K, Kim YJ, Kim YH, Roh JN, Nam JM, Kim PY, Ryu WS, Lee SH, Yoon BW. (2012) Lithium pretreatment reduces brain injury after intracerebral hemorrhage in rats. Neurol Res. 34, 447-54.

Khasraw M, Ashley D, Wheeler G, and Berk M (2012) Using lithium as a neuroprotective agent in patients with cancer. BMC Medicine. 10, 131-137.

Kumar AP, Ryan C, Cordy V, Reynolds WF (2005) Inducible nitric oxide synthase expression is inhibited by myeloperoxidase. J. Biology and Chemistry. 13, 42-53.

Lechner M, Lirk P, Rieder J (2005) Induceble nitric Oxide Synthase (iNOS) in tumor biology: The two side of the same coin. J. cancer biology. 15, 277-289.

Lenox RH, Wang L (2003) Molecular basis of lithium action: integration of lithium-responsive signaling and gene expression networks. Molecular Psychiatry. 8, 135–144.

Li, Q Li H, Roughton K, Wang X, Kroemer G, Blomgren K, Zhu C (2010) Lithium reduces apoptosis and autophagy after neonatal hypoxia-ischemia. J. Neurosci. 10, 2041-4889.

Madigan MT, Martnko JM, Dunlap PV, Clark DP (2009) Brock Biology of microorganisms. Benjamin commings. 12th ED. 479.

Mampuru LJ, Abotsi EK, Wachira SJM (1999) Calyculin-A potentiates growth and apoptotic effects of lithium in HL-60 cells. J Trace Microprobe Tech 17, 367–378.

Matsebatlela T, Gallicchio V, Becker R (2012) Lithium Modulates Cancer Cell Growth, Apoptosis, Gene Expression and Cytokine Production in HL-60 Promyelocytic Leukaemia Cells and Their Drug-Resistant Sub-clones. Biol Trace Elem Res. 149, 323–330.

Matsebatlela TM, Mogodiri RK, Hart DA, Gallicchio VS, Becker RW (2000) Resistance to lithium-induced apoptosis in a lithium tolerant clone of HL-6 promyelocytes. J. Trace and Microprobe Techniques. 18(1), 163-170.

Moynagh PN (2005) The NF-κB pathway. Journal of Cell Science. 118, 4389-4392.

May MJ, Ghosh S (1997) Rel/NF-κB and IκB proteins: an overview. *seminars in* Cancer Biology, Vol 8, 63–73.

McKellar G, Madhok R, Singh G (2007) The problem with NSAIDs: what data to believe? Curr Pain Headache Rep. 11, 423–427.

Peakman M, Vergani D (1997). Basic and clinical immunology. *Churchill Livingstone*. 12-13.

Pizarro JG, Yeste-Velasco M, Rimbau V, Casadesúsd G, Smith MA , Pallàsa M, Folch J, Camins A (2008) Neuroprotective effects of SB-415286 on hydrogen peroxide-induced cell death in B65 rat neuroblastoma cells and neurons. International Journal of Developmental Neuroscience. 26, 269–276.

Peakman, M., and Vergani, D.(1997). Basic and clinical immunology. Churchill liningstone.NY, London, Tokyo. 2nd ED, 12-13.

Plowden J, Renshaw-Hoelscher M, Engleman C, Katz J, Sambhara S (2004) Innate immunity in aging: impact on macrophage function. Ltd/Anatomical. 161-167.

Perkins ND, Schmid RM, Duckett CS, Leung K, Rice NR, Nabel GJ (1992) Distinct combinations of NF-kB subunits determine the specificity of transcriptional activation. Proc. Natl. Acad. Sci. USA 89,1529–1533.

Quiroz JA, Gould TD, Manji HK, (2004) Molecular effects of lithium. The International Journal of Neuropsychopharmacology. 8, 259–272.

Reuter S, Gupta SC, Chaturvedi MM, Aggarwal (2010) Oxidative stress, inflammation, and cancer: How are they linked? J. free rad-biomed. 49: 1603–1616.

Ross JA, Auger MJ (2002) The biology of the macrophage. Burke B and Lewis CE, editors. Oxford: Medical Publications. 2nd ED.1–72.

Sinha D, Wang Z, Ruchalski KL, Levine JS, Krishnan S, Lieberthal W, Schwartz JH, Borkan SC (2004) Lithium activates the Wnt and phosphatidylinositol 3-kinase Akt signalling pathways to promote cell survival in the absence of soluble survival factors. *J. Physiol Renal Physiol*. 288, F703–F713.

Strunecká A, Patočka J, Sárek M (2005) How does lithium mediate its therapeutic effects. J. Appl. Biomed. 3, 25-35.

Shavali S, Combs CK, Ebadi M (2006) Reactive Macrophages Increase Oxidative Stress and Alpha-Synuclein Nitration During Death of Dopaminergic Neuronal Cells in Co-Culture: Relevance to Parkinson's Disease. J. Neurochemical Research. doi: 10.1007/s11064-005-9233-x. Accessed 1 January 2006.

Suganthi M, Sangeetha G, Gayathri G, Sankar BR (2012) Biphasic Dose-Dependent Effect of Lithium Chloride on Survival of Human Hormone-Dependent Breast Cancer Cells (MCF-7). Biol Trace Elem Res 150, 477–486.

Townsend DM, Tew KD, Tapiero H (2003) The importance of glutathione in human disease. Biomedicine & Pharmacotherapy 57, 145–155.

Tim CP, Linch DC, Khwaja A (2011) apoptosis through a pathway involving glycogen synthase kinase-3 and Bax Growth factor withdrawal from primary human erythroid progenitors induces. J. ASH. 98, 1374-1381.

Taylor PR, Martinez-Pomares L, Stacey M, Lin HH, Brown GD, Gordon S (2005) macrophage receptors and immune recognition. Annu. Rev. Immunol. 23, 901–44

Udalova IA, Richardson A, Denys A, Smith C, Ackerman H, Foxwell B, Kwiatkowski D (2000) Functional Consequences of a Polymorphism Affecting NF-Kb p50-p50 Binding to the *TNF* Promoter Region. Mol. Cell. Biol. 20(24), 9113.

Valko M, Leibfritz D, Moncola J, Cronin MTD, Mazura M, Telser J, (2007) Free radicals and antioxidants in normal physiological functions and human disease. *J. Biochemistry & Cell Biology*: 39, 44–84.

Vogiatzi, G., Tousoulis, D., and Stefanadis, C (2009) The Role of Oxidative Stress in Atherosclerosis. J. Cardiol 50, 402-409.

Valko M*,* Leibfritz D, Moncola J, Cronin MTD, Mazura M, Telser J (2006) Free radicals and antioxidants in normal physiological functions and human disease. The International Journal of Biochemistry & Cell Biology 39 (2007), 44–84.

Williams RSB, Harwood AJ (2000) Lithium therapy and signal transduction. J. Viewpoint. 21, 61-64.

Xu W, Roos A, Daha MR, van Kooten C (2006) Dendritic cell and macrophage subsets in the handling of dying cells. Immunobiology 211, 567–575.

Yeste-Velasco M, Folch J, Jiménez A, Rimbau V, Pallàs M, Camins A (2008) GSK-3β inhibition and prevention of mitochondrial apoptosis inducing factor release are not involved in the antioxidant properties of SB-415286. J. Pharmacology. 588, 239–243.

Zhang M, Jin W, Zhou X, Yu J, Lee AJ, Sun S (2008) Deregulation of Tpl2 and NF-κB signaling and induction of macrophage apoptosis by the anti-depressant drug lithium. J. cellular signalling. 21, 559- 566.